CHEM**MED**CHEM

CHEMISTRY ENABLING DRUG DISCOVERY

Accepted Article

Authors: Jakub Modranka, Jiahong Li, Anastasia Parchina, Michiel Vanmeert, Shrinivas Dumbre, Mayla Salman, Hannu Myllykallio, Hubert F. Becker, Roeland Vanhoutte, Lia Margamuljana, Hoai Nguyen, Rania Abu El Asrar, Jef Rozenski, Piet Herdewijn, Steven Dejonghe, and Eveline Lescrinier

A Journal of

ChemPubSoc Europe

FULL PAPER

Synthesis and structure-activity relationship studies of benzo[b][1,4]oxazin-3(4H)-one analogues as inhibitors of mycobacterial thymidylate synthase X

Jakub Modranka,[‖],[a] Jiahong Li,[‖],[a] Anastasia Parchina,[‖],[a] Michiel Vanmeert,[a] Shrinivas Dumbre,[a] Mayla Salman,[b] Hannu Myllykallio,[b] Hubert F. Becker,[b,c] Roeland Vanhoutte,[‡,d] Lia Margamuljana,[a] Hoai Nguyen,[a] Rania Abu El Asrar,[a] Jef Rozenski,[a] Piet Herdewijn,[a] Steven De Jonghe,[*,†,e] and Eveline Lescrinier*[a]

[a]	Dr. J. Modranka (0000-0001-9239-8535), Dr. J. Li, Dr. A. Parchina, Mr. M. Vanmeert (0000-0001-5810-4935), Dr. S. Dumbre (0000-0002-1237-9586), Mrs. L. Margamuljana, Mrs. H. Nguyen, Ms. R. Abu El Asrar, Prof. J. Rozenski (0000-0001-9624-5536), Prof. P. Herdewijn (0000-0003-3589-8503), Dr. S. De Jonghe, Prof. E. Lescrinier (0000-0001-7066-4329) Medicinal Chemistry, Rega Institute for Medical Science KU Leuven Herestraat 49 – PO Box 1030, BE-3000 Leuven, Belgium E-mail: Steven.Dejonghe@kuleuven.be; Eveline.Lescrinier@kuleuven.be
[b]	Dr. M. Salman, Prof. H. Myllykallio (0000-0002-0541-1197), H.F. Becker (0000-0003-3136-6075) Laboratory of Optics and Biosciences INSERM U 696- CNRS UMR 7645 -Ecole Polytechnique Route de Saclay, 91128 Palaiseau Cedex, France
[c]	Prof. H.F. Becker (0000-0003-3136-6075) Faculté des Sciences et Ingénierie Sorbonne Université 4 place Jussieu 75005 Paris, France
‖	These authors contributed equally.
†	Present affiliation: Laboratory of Virology and Chemotherapy, Rega Institute for Medical Research, KU Leuven, Herestraat 49 – box 1043 , 3000 Leuven, Belgium.
‡	Present affiliation: Laboratory of Chemical Biology, KU Leuven, O&N I Herestraat 49 - box 802, 3000 Leuven, Belgium.

Supporting information for this article is given via a link at the end of the document.

Abstract: Since the discovery of a flavin-dependent thymidylate synthase (ThyX or FDTS), that is absent in humans but crucial for DNA biosynthesis in a diverse group of pathogens, the enzyme has been pursued for the development of new antibacterial agents against *Mycobacterium tuberculosis*, the causative agent of the widespread infectious disease tuberculosis (TB). In response to a growing need for more effective anti-TB drugs, we have built upon our previous screening efforts and report here an optimization campaign of a novel series of inhibitors with a unique inhibition profile. The inhibitors display competitive inhibition towards the methylene tetrahydrofolate cofactor of the enzyme, enabling us to generate a model of the compounds bound to their target and offering insights into their structure–activity relationships.

Introduction

Tuberculosis (TB) is a contagious-infectious disease caused by the bacterium *Mycobacterium tuberculosis*. Currently, it is the ninth leading cause of death worldwide and the leading cause from a single infectious agent.[1] The prognosis for patients with tuberculosis improved dramatically with the introduction of antitubercular drugs (such as rifampicine, isoniazid, pyrazinamide and ethambutol).[2] Despite having these treatment options, according to the latest report of the World Health Organisation (WHO), *M. tuberculosis* still caused an estimated 1.7 million deaths in 2016. In addition, an estimated 10.4 million people fell ill with tuberculosis.[1] Recently, two new antitubercular drugs (bedaquiline[3] and delamanid[4]) received marketing approval. However, the emergence of multidrug-resistant (MDR), extensively drug-resistant (XDR) and even totally drug-resistant (TDR) *M. tuberculosis* strains remains a major threat to public health.[5] Consequently, there is an urgent demand for new antituberculosis drugs acting on novel mycobacterial targets.

Thymidylate synthase (ThyA) catalyzes the *de novo* synthesis of thymidine-5'-monophosphate (TMP) via reductive methylation of 2'-deoxyuridine-5'-monophosphate (dUMP). ThyA uses *N*-5,*N*-10-methylene tetrahydrofolic acid (CH_2H_4folate) both as one carbon and hydride donor, whereby dihydrofolate (DHF) is formed. The catalytic activity of ThyA is coupled to the action of two other enzymes. Dihydrofolate reductase (DHFR) mediates the reduction of DHF to tetrahydrofolate (H_4folate), which is further subjected to remethylenation catalyzed by serine hydroxymethyltransferase (SHMT) to regenerate the CH_2H_4folate pools. Thymidine-5'-monophosphate is readily phosphorylated to thymidine-5'-triphosphate (TTP), one of the four building blocks required for the biosynthesis of DNA.[6] Several human pathogens

FULL PAPER

lack the genes encoding for ThyA and DHFR, but are still fully viable in thymidine-deficient media. Genomic analysis led to the discovery of the *thyX* gene which encodes for the ThyX-protein, a flavin-dependent thymidylate synthase (FDTS) which is absent in humans.[7] ThyX uses CH_2H_4folate only as one-carbon donor, with reduced flavin adenine dinucleotide ($FADH_2$) serving as a hydride donor. ThyX enzymes are NAD(P)H-oxidases since catalysis requires the presence of NAD(P)H to furnish sufficient amounts of $FADH_2$ via reduction of FAD.[8] Furthermore, ThyX shows no structural or sequence similarity with ThyA.[9] While some pathogens solely rely on ThyX, *M. tuberculosis* carries conserved genes encoding for ThyA as well as for ThyX.[7] The *thyX*-gene is required and essential for mycobacterial growth and survival within macrophages, making ThyX a promising antimycobacterial drug target.[10] Despite this, only a limited number of ThyX inhibitors is known (Figure 1).[11] Structural variation of the uracil moiety of the natural substrate dUMP afforded a series of 5-alkynyl dUMP analogues, from which the most potent congener (compound **1**), displayed an IC_{50} value of 0.9 μM against mycobacterial ThyX.[12]
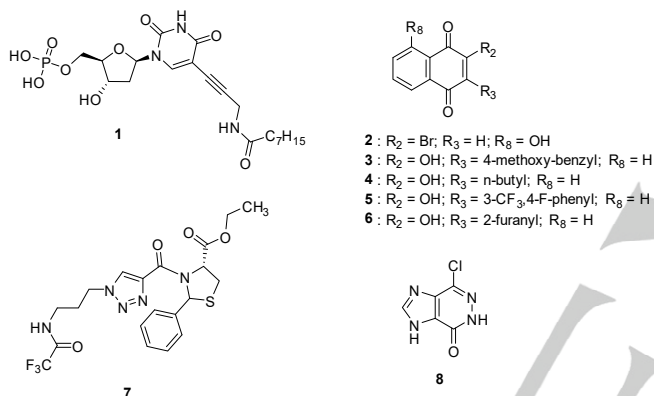
cells. Therefore, quinones are not desirable scaffolds in medicinal chemistry.[15] A library of thiazolidine derivatives has been prepared and evaluated as inhibitors of viral *PBCV-1* ThyX. The most potent congener (compound **7**) was endowed with an IC_{50} value of 0.057 μM.[16] In an effort to obtain non-substrate inhibitors, a virtual screening campaign of the ZINC database against mycobacterial ThyX was performed. The most potent congener was an imidazo[4,5-d]pyridazine analogue (compound **8**) that, however, displayed only 29% inhibition at 100 μM.[17]

Because of the potential of ThyX as antibacterial drug target and the lack of drug-like small-molecule ThyX inhibitors, we recently embarked on a high-throughput screening (HTS) campaign of commercially available compound libraries in the search for novel and drug-like mycobacterial ThyX inhibitors. It led to the discovery of B1-PP146 (compound **9**, Figure 2) as a tight-binding mycobacterial ThyX inhibitor with an IC_{50} of 0.71 μM.[18] Screening of structurally related, commercially available analogues led to the discovery of compound **10**, endowed with an IC_{50} value of 0.9 μM. As the *N*-carboxamide-piperazine substructure of compound **10** allows for more and easier structural variation than the *N*-pyrimidinyl-piperazine moiety of **9**, compound **10** was selected as starting point for an optimization campaign. In this manuscript, we describe our medicinal chemistry efforts in order to study the structure-activity relationship of these benzoxazine analogues as inhibitors of mycobacterial ThyX.
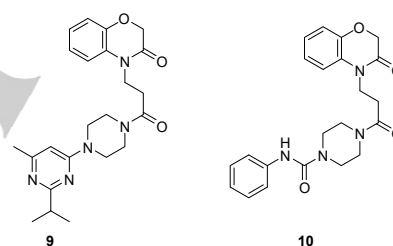

Figure 1. Inhibitors of ThyX.

2 : R_2 = Br; R_3 = H; R_8 = OH
3 : R_2 = OH; R_3 = 4-methoxy-benzyl; R_8 = H
4 : R_2 = OH; R_3 = n-butyl; R_8 = H
5 : R_2 = OH; R_3 = 3-CF_3,4-F-phenyl; R_8 = H
6 : R_2 = OH; R_3 = 2-furanyl; R_8 = H

Figure 2. Benzo[b][1,4]oxazin-3(4H)-ones as mycobacterial ThyX inhibitors.

However, the presence of the polar phosphate moiety precludes its further development into derivatives with *in vitro* antimycobacterial activity. 2-Bromo-8-hydroxy-1,4-naphthoquinone (compound **2**) and 2-hydroxy-3-(4-methoxybenzyl)-1,4-naphthoquinone (compound **3**) have been identified as inhibitors of ThyX from *Paramecium bursaria chlorella virus-1* (*PBCV-1*). In addition, these compounds inhibit ThyX proteins from other microorganisms, including *M. tuberculosis*, *H. pylori* and *C. trachomatis*. Moreover, compound **2** displays antibacterial activity in a genetically modified *E. coli* strain harboring the ThyX gene.[13] Further optimization of this class of compounds as ThyX inhibitors from *H. pylori* led to the discovery of new analogues with improved ThyX inhibition and antibacterial activity.[14] Moreover, three representatives displayed promising activity in a mouse model of *H. pylori* infection.[14] The authors did not observe any cytotoxicity, mitochondrial toxicity or *in vivo* toxicity with these quinone analogues. However, it is well known that quinones act as Michael acceptors and can cause cellular damage by alkylation of cellular proteins and/or DNA. In addition, quinones are highly redox active molecules that can lead to the formation of reactive oxygen species (ROS), which can cause severe oxidative stress within

Results and Discussion

Chemistry

The synthesis of *N*-phenylpiperazine-1-carboxamide analogues **17a-i** with structural variation of the phenyl part of the bicyclic benzo[b][1,4]oxazin-3(4H)-one scaffold was accomplished as shown in Scheme 1. Commercially available 2H-benzo[b][1,4]oxazin-3(4H)-one derivatives **11a-h** were *N*-alkylated with ethyl 3-bromopropionate under alkaline conditions.[19] Saponification of the ethyl ester moiety of **12a-h** with lithium hydroxide furnished the carboxylic acids **13a-h**. *N*-Phenylpiperazine-1-carboxamide **16** was synthesized by reaction of *tert*-butyl piperazine-1-carboxylate **14** with phenyl isocyanate, followed by acidic deprotection of the Boc group.[20] Finally, reaction of acids **13a-h** and amine **16** with O-(1H-6-chlorobenzotriazole-1-yl)-1,1,3,3-tetramethyluronium hexafluorophosphate (HCTU) as coupling reagent afforded the desired compounds **17a-h**.

2

Scheme 1. Reagents and conditions : a) ethyl 3-bromopropionate, K2CO3, DMF, 80°C; b) LiOH, THF, 60°C; c) PhNCO, THF, rt; d) TFA, 0 °C; e) HCTU, DIPEA, DMSO, rt.
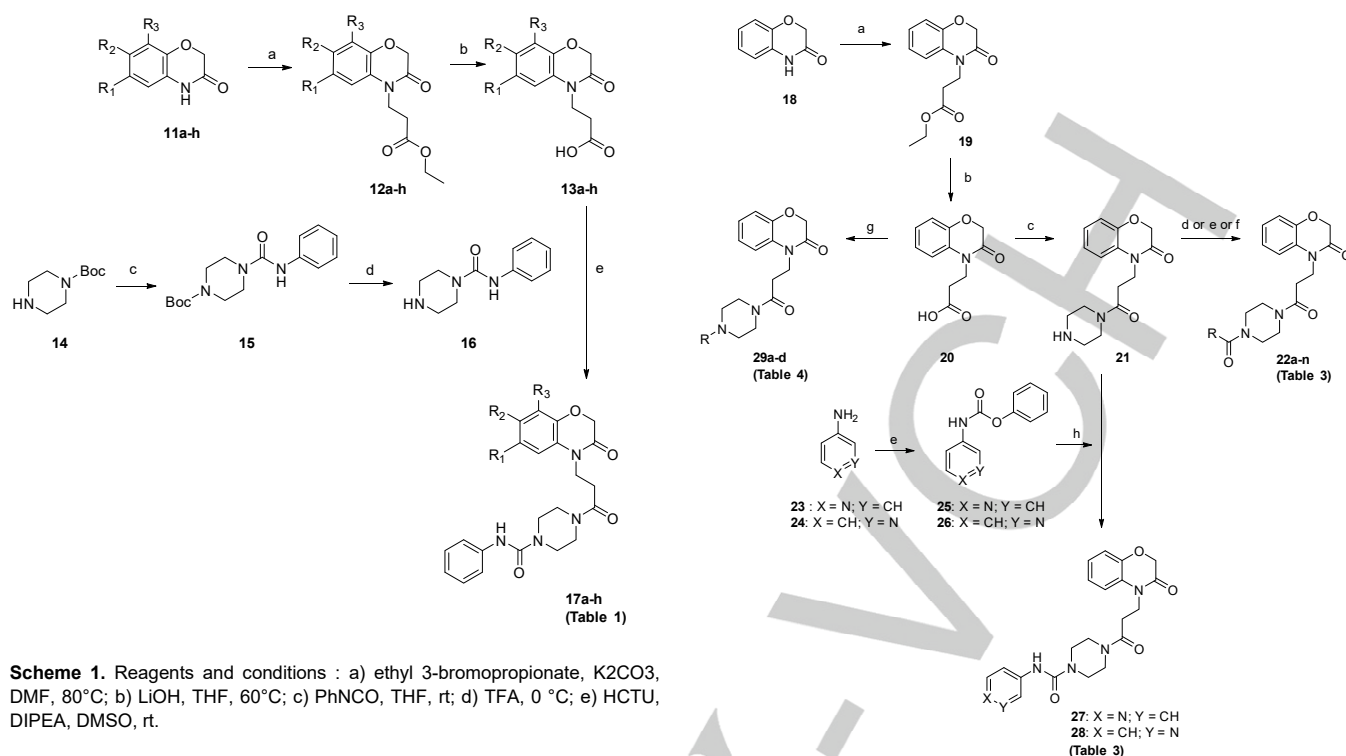
For the synthesis of a library with structural variation of the terminal aryl group, a slightly modified scheme was used (Scheme 2). Alkylation of **18**, followed by alkaline hydrolysis of the ester moiety, furnished acid **20**. DCC-mediated amide formation afforded compound **21**, as key intermediate from which structural variation could easily be introduced. Reaction with a series of isocyanates gave access to a set of urea derivatives **22a-l**. Alternatively, coupling of **21** with phenyl chloroformate or phenylacetyl chloride furnished carbamate **22m** and amide **22n**, respectively. For the synthesis of pyridine-containing urea derivatives **27** and **28**, 4- and 3-aminopyridine (compounds **23** and **24**, respectively) were first coupled with phenylchloroformate yielding carbamates **25** and **26**, respectively. Condensation with piperazine analogue **21** furnished derivatives **27** and **28**, respectively. Because of the commercial availability of a number of piperazine building blocks, carboxylic acid **20** was easily converted in one step to the corresponding piperazine analogues **29a-d**.

The synthesis of analogues with variation in the linker moiety between the benzo[b][1,4]oxazin-3(4H)-one core and the piperazine moiety was effected as shown in Scheme 3. Alkylation of **18** with the appropriate alkyl bromides gave access to compounds **30** and **31**. Hydrolysis of the ethyl ester group, followed by coupling with piperazine and phenylisocyanate afforded final compounds **32** and **33**. For the synthesis of branched-chain derivatives, a similar methodology was applied. Alkylation of **18** with suitable alkyl bromides gave compounds **34** and **35**. Saponification of the ester moiety, followed by reaction with *N*-phenylcarboxamide piperazine **16** yielded the desired derivatives **36** and **37**.

Scheme 2. *Reagents and conditions :* a) ethyl 3-bromopropionate, K2CO3, DMF, 90°C; b) LiOH, THF, 45°C; c) DCC, HOBt, piperazine, rt; d) RNCO, DMF, rt; e) PhOC(O)Cl, DIPEA, DMF, rt (for **22m**); f) PhCH2C(O)Cl, DIPEA, DMF, rt (for **22n**); g) R-piperazine, HCTU, DIPEA, rt; h) DIPEA, DMF, rt.

Scheme 3. *Reagents and conditions.* a) ethyl bromoacetate (for **30**) or ethyl 4-bromobutyrate (for **31**), K2CO3, DMF, 90°C; b) (i) LiOH, H2O, THF; 45°C; (ii) DCC, HOBT, piperazine, DMF, rt; (iii) PhNCO, DMF, rt; c) methyl 3-bromobutanoate (for **34**) or methyl 3-bromo-2-methylpropanoate (for **35**), K2CO3, DMF, 90°C; d) (i) LiOH, H2O, THF, 45 °C; (ii) DCC, HOBT, *N*-phenylpiperazine-1-carboxamide, DMF; e) *tert*-butyl 4-(3-propyl)piperazine-1-carboxylate, K2CO3, DMF, 65 °C; f) (i) TFA, rt; (ii) PhNCO, THF, rt

To have the piperazine ring linked to the benzo[b][1,4]oxazin-3(4H)-one scaffold by an alkyl chain (rather than an amide bond), *tert*-butyl 4-(3-bromopropyl)piperazine-1-carboxylate was reacted

3

FULL PAPER

with **18** in the presence of potassium carbonate yielding intermediate **38**. Acidic removal of the Boc protecting group and condensation with phenyl isocyanate afforded target compound **39**.
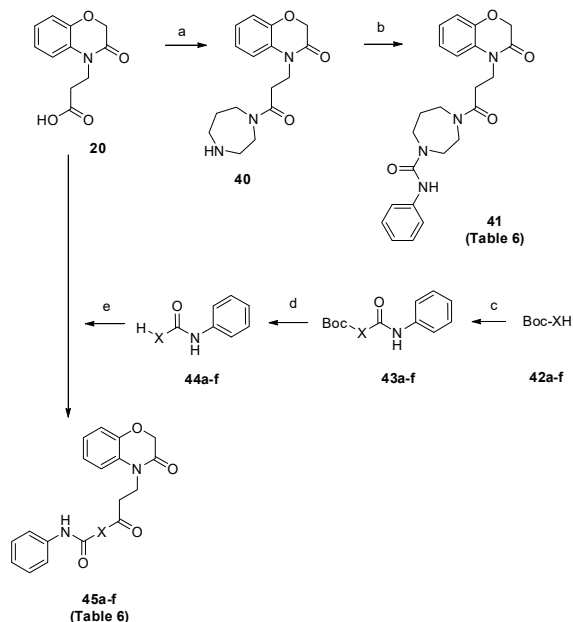
Scheme 4. *Reagents and conditions* : a) DCC, HOBt, homopiperazine, DMF; b) phenylisocyanate, DMF; c) PhNCO, THF; d) TFA, CH₂Cl₂; e) HCTU, DIPEA, DMSO.

Modifications in the piperazine motif were introduced as shown in Scheme 4. For the synthesis of the homopiperazine analogue **41**, a stepwise approach starting from compound **20** was followed, consisting of amide coupling and urea formation, yielding the 1,4-diazepine analogue **41**. On the other hand, for the methyl-substituted piperazine analogues **45a-b**, the amino-piperidine derivatives **45c-d** and the amino-pyrrolidine congeners **45e-f**, a slightly different methodology was used. The free amino group of the Boc protected building blocks **42a-f** was coupled with phenylisocyanate, followed by acidic cleavage of the Boc group. Finally, amide coupling of **44a-f** with **20** yielded a series of analogues **45a-f** with structural variation of the piperazine moiety. Scaffold modified analogues were prepared from appropriate, commercially available building blocks (Scheme 5). The synthesis of pyrido-fused oxazine analogues started from the commercially available 2H-pyrido[3,2-b][1,4]oxazin-3(4H)-one **46** and 1H-pyrido[2,3-b][1,4]oxazin-2(3H)-one **47**. *N*-alkylation, followed by ester hydrolysis and amide coupling yielded the desired analogues **48** and **49**. A number of derivatives with substituents at position 2 of the oxazine ring were also prepared. 2-methyl-2H-benzo[b][1,4]oxazin-3(4H)-one **50** is commercially available, whereas building blocks with a mono- (compound **51**) or difluorinated (compound **52**) oxazine moiety were synthesized according to literature procedures.[21] Applying the standard reaction conditions (*N*-alkylation, ester hydrolysis, amide formation) yielded compounds **53**, **54** and **55**. Final derivatives **58** and **59** were prepared in a similar way starting from benzo[b][1,4]thiazin-3(4H)-one **56** or 3,4-dihydroquinolin-2(1H)-one **57**. To have access to a 3,4-dihydroquinoxaline based analogue, *tert*-butyl 3-oxo-3,4-dihydroquinoxaline-1(2H)-

carboxylate **60** (synthesized according to literature procedure[22]) was selected as starting material. Alkylation, followed by saponification of the ester residue and formation of an amide bond yielded the desired compound **61**. Unfortunately, upon cleavage of the Boc protecting group under acidic conditions, a concomitant oxidation of the 3,4-dihydroquinoxalin-2(1H)-one moiety took place yielding the quinoxalin-2(1H)-one analogue **62**. The benzoxazole congener **64** was easily obtained by reaction of **63** with *N*-phenylpiperazine-1-carboxamide **16**. A benzoxazine analogue lacking the 2-oxo functionality (compound **66**) was accessible via alkylation of **65**, followed by ester hydrolysis and amide coupling.
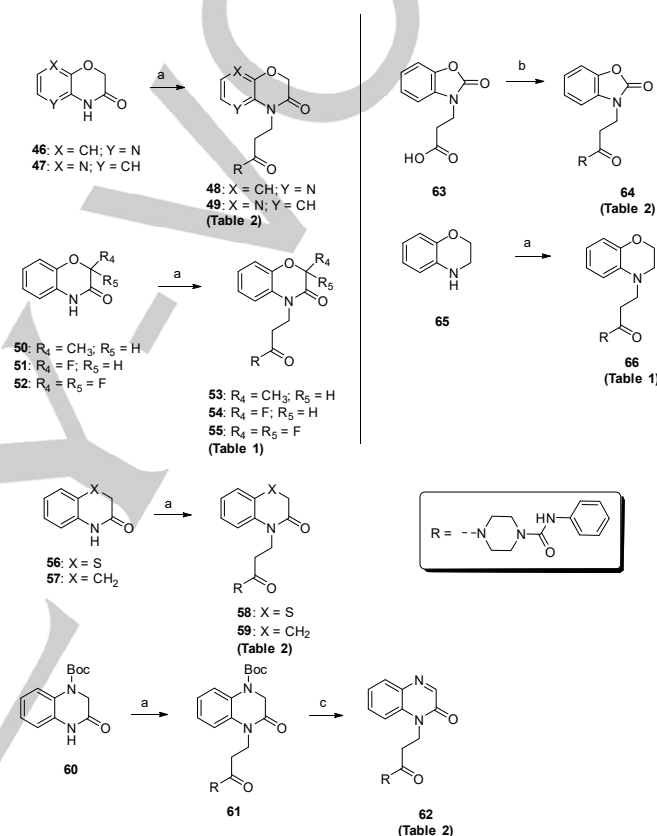

Scheme 5. *Reagents and conditions* : a) (i) ethyl 3-bromopropionate, K₂CO₃, DMF; (ii) LiOH, THF; (iii) DCC, HOBt, *N*-phenylpiperazine-1-carboxamide, DMF; b) DCC, HOBt, *N*-phenylpiperazine-1-carboxamide, DMF; c) TFA, CH₂Cl₂.

Mycobacterial ThyX inhibition and structure-activity relationship studies

To investigate the SAR in a systematic way, hit compound **10** was divided in different areas, and each of these substructures was subjected to structural modifications (Figure 3). In a primary screening, all compounds were tested at a concentration of 5 μM as potential inhibitors of mycobacterial ThyX in a spectrophotometric based assay. Folinic acid (also known as leucovorin) (50 μM) was included as a reference to scale the inhibitory activity of tested compounds. At a concentration of 50 μM, folinic acid inhibited ThyX enzymatic activity by 80 %. Hence, compounds with relative inhibition of more than 1 in this study, inhibited the ThyX activity more than 80% at 5 ☐M. For the hit compound and its derivatives that had a relative inhibition of at least 1, the concentration to obtain 50% of the maximal inhibition

4

FULL PAPER

(IC$_{50}$) was determined using full dose-response curves. All selected compounds were able to fully inhibit the enzymatic activity of ThyX in the selected conditions.
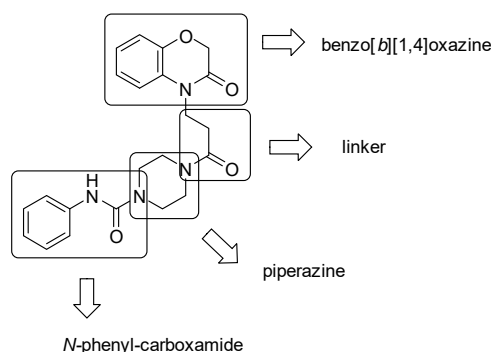
Figure 3. Division of compound **10** in different substructures

SAR of the benzo[b][1,4]oxazin-3(4H)-one moiety : substitution pattern

The influence of substitution of the phenyl moiety of the benzo[b][1,4]oxazin-3(4H)-one core on ThyX inhibition was evaluated. The introduction of small electron-withdrawing groups, such as nitro and acetyl groups (compounds **17c** and **17d**, respectively) and electron-donating groups, such as a methyl moiety (compound **17c**) yielded analogues that were completely devoid of mycobacterial ThyX inhibition. On the other hand, substituting the phenyl ring with a chlorine at position 6 afforded compound **17a**, which was equipotent with hit compound **10** (relative inhibition of 0.7 at 5 µM). The chlorinated regioisomer (compound **17h**) was endowed with less inhibitory activity against ThyX (relative inhibition of 0.47 at 5 µM), whereas a fluorine at position 7 afforded compound **17g** which was still endowed with reasonable ThyX inhibition (IC$_{50}$ = 1.75 µM). A dichlorinated analogue (compound **17f**) was completely devoid of ThyX inhibition. A sterically demanding phenyl group (compound **17e**) led to a complete loss of ThyX inhibition. The substitution pattern of the oxazine moiety was also explored. Introduction of a methyl or fluorine(s) (compounds **53-55**) completely abolished ThyX inhibition. Reduction of the lactam functionality of compound **10** to an amine afforded compound **66**, which was much less active as a ThyX inhibitor (relative inhibition of 0.35 at 5 µM). Overall, this SAR study reveals that very little variation is tolerated on the benzo[b][1,4]oxazin-3(4H)-one moiety with respect to ThyX inhibition.

Cmpd#	R$_1$	R$_2$	R$_3$	R$_4$	R$_5$	rel. inhibition @ 5 µM	IC$_{50}$ (µM)
10 (Hit)	H	H	H	H	H	0.70	0.93 (0.17)[b]
17a	Cl	H	H	H	H	0.72	ND[a]
17b	CH$_3$	H	H	H	H	0.28	ND[a]
17c	NO$_2$	H	H	H	H	0	ND[a]
17d	COCH$_3$	H	H	H	H	0.10	ND[a]
17e	Ph	H	H	H	H	0.04	ND[a]
17f	Cl	H	Cl	H	H	0.19	ND[a]
17g	H	F	H	H	H	0.81	ND[a]
17h	H	Cl	H	H	H	0.47	ND[a]
53	H	H	H	CH$_3$	H	0	ND[a]
54	H	H	H	F	H	0.15	ND[a]
55	H	H	H	F	F	0.15	ND[a]
66	-	-	-	-	-	0.35	ND[a]

[a]ND : Not determined. [b]Standard deviation given between parentheses

SAR of the benzo[b][1,4]oxazin-3(4H)-one moiety : scaffold modification

As pyridine is a known bioisoster of benzene, two pyrido-oxazine analogues were prepared. Whereas the pyrido[3,2-b][1,4]oxazin-3(4H)-one congener **48** was endowed with promising ThyX inhibition (IC$_{50}$ = 1.72 µM), its isomeric pyrido[2,3-b][1,4]oxazin-2(3H)-one analogue **49** completely lacks ThyX inhibition, pointing towards a crucial role of the position of the nitrogen atom. Other scaffold variations focused on the oxazine moiety and included a benzo[b][1,4]thiazine (compound **58**) and tetrahydroquinoline scaffold (compound **59**), which were both found to be inactive. The quinoxaline analogue **62** exhibited potent ThyX inhibition, displaying an IC$_{50}$ value of 1.46 µM. Converting the 6-membered oxazine moiety into a five-membered ring yielded the benzo[d]oxazol-2(3H)-one derivative **64**, which was completely devoid of ThyX inhibition.

5

FULL PAPER

Table 2. SAR of scaffold modified benzoxazine analogues.

Cmpd#	A	B	X	rel. inhibition @ 5 µM	IC$_{50}$ (µM)
10 (Hit)	CH	CH	O	0.70	0.93 (0.17)[b]
49	N	CH	O	0	ND[a]
48	CH	N	O	1.24	1.72 (0.06)[b]
58	CH	CH	S	0.16	ND[a]
59	CH	CH	CH$_2$	0	ND[a]
62	-	-	-	1.13	1.46 (0.05)[b]
64	-	-	-	0.06	ND[a]

[a]ND : Not determined. [b]Standard deviation given between parentheses.

SAR of the N-phenylcarboxamide moiety

To probe into the optimal substitution pattern of the terminal phenyl ring, a variety of small substituents (e.g. halogens, methyl, methoxy, cyano and acetyl) were introduced. As can be derived from the data in Table 3, quite some structural variety is tolerated at this position, as these different analogues (**22a-i**) display a relative inhibition between 0.44 and 0.95 at 5 µM, compared to 50 □M folinic acid in identical conditions. For a selected number of derivatives, IC$_{50}$ values were obtained. Thienyl and pyridyl are both known isosters of the phenyl and therefore compounds **22j**, **27** and **28** were also prepared. Only compound **27** was more active than compound **10** at 5 □M (relative inhibition of 1.19, IC$_{50}$ = 2.38 □M).

Instead of the terminal phenyl, a benzyl and phenethyl congener were also prepared. Although an elongation with one carbon (compound **22k**) still gives a potent ThyX inhibitor (relative inhibition of 0.83), further elongation by two carbons (compound **22l**) gave rise to a diminished ThyX inhibition. To assess the importance of the urea moiety, the corresponding carbamate (compound **22m**) and amide (compound **22n**) were both prepared. The carbamate was still endowed with reasonable ThyX inhibition (relative inhibition of 0.5), whereas the amide is much less active as a ThyX inhibitor.

Rather than directly attaching a carbonyl to the piperazine moiety (generating a urea, carbamate or amide), a number of compounds was synthesized in which a methylene linker between the carbonyl group and the piperazine nitrogen was inserted (Table 4). This makes the amine group to have basic properties, which should have an impact on its biological activity, solubility and permeability. Several congeners within this family were endowed with ThyX inhibitory activity (e.g. compounds **29a** and **29c**, both having a heteroaromatic substituent), and especially the *N*-methyl-*N*-phenylpropionamide derivative **29d** displayed potent ThyX inhibition with an IC$_{50}$ value of 0.69 µM

Table 3. SAR of the *N*-phenylcarboxamide moiety.

Cmpd#	R	rel. inhibition @ 5 µM	IC$_{50}$ (µM)
10 (hit)		0.70	0.93 (0.17)[b]
22a		0.09	ND[a]
22b		0.23	ND[a]
22c		0.58	ND[a]
22d		0.62	ND[a]
22e		0.76	ND[a]
22f		0.61	ND[a]
22g		1.06	2.04 (0.08)[b]
22h		0.44	ND[a]
22i		0.77	ND[a]
22j		0.52	ND[a]
22k		0.83	ND[a]
22l		0.54	ND[a]
22m		0.52	ND[a]
22n		0.31	ND[a]
27		1.19	2.38 (0.08)[b]
28		1.13	3.56 (0.09)[b]

[a]ND : Not determined. [b]Standard deviation given between parentheses.

6

Table 4. SAR of the piperazinyl-acetamide derivatives.

Cmpd#	R	rel. inhibition @ 5 µM	IC$_{50}$ (µM)
29a		0.89	ND[a]
29b		0.53	ND[a]
29c		0.99	ND[a]
29d		1.37	0.69 (0.08)[b]

[a]ND : Not determined. [b]Standard deviation given between parentheses.

SAR of the propanoyl linker
Subsequently, the importance of the linker between the oxazine and the piperazine moiety was evaluated (Table 5). Shortening (compound **32**), elongation (compound **33**) or branching (compounds **36** and **37**) of the propanoyl linker led inevitably to completely inactive compounds. Reduction of the amide group yielded a derivative with a *n*-propyl linker (compound **39**) that similarly showed a complete loss of ThyX inhibition.

Table 5. SAR of linker modified analogues

Cmpd#	X	rel. inhibition @ 5 µM	IC$_{50}$ (µM)
10 (Hit)		0.70	0.93 (0.17)[b]
32		0	ND[a]
33		0	ND[a]

36	0	ND[a]
37	0	ND[a]
39	0	ND[a]

[a]ND : Not determined. [b]Standard deviation given between parentheses

SAR of the piperazine moiety
As shown in Table 6, substituting the piperazine ring of hit compound **10** for a 1,4-diazepine ring (homopiperazine analogue **41**) resulted in a completely inactive derivative. Upon introducing a methyl group on the piperazine ring (compounds **45a** and **45b**), the exact position on the piperazine ring plays a determining role in its ThyX inhibitory activity. The presence of a methyl closer to the benzoxazine core afforded compound **45b** that was endowed with potent ThyX inhibition (relative inhibition of 0.88). On the other hand, when the same methyl group was introduced closer to the urea functionality (compound **45a**), a decreased potency was observed when compared to the unsubstituted congener **10**. To broaden the SAR investigation, the piperazine moiety was replaced by other nitrogen-containing saturated heterocycles. The amino-piperidine congener **45c** displayed better activity against mycobacterial ThyX (IC$_{50}$ = 0.88 µM), when compared to the parent piperazine analogue **10**. The closely related amino-piperidine congener **45d** lacks activity. A similar profile was found in the aminopyrrolidine subseries. When the exocyclic amino group of aminopyrrolidine was derivatised as a urea (compound **45e**), the compound was endowed with substantial ThyX inhibition (IC$_{50}$ = 2.95 µM). On the other hand, when the exocyclic amino group was connected to the propanyl linker (compound **45f**), it was completely devoid of inhibitory activity.

Table 6. SAR of the piperazine moiety.

Cmpd#	X	rel inhibition @ 5 µM	IC$_{50}$ (µM)
10 (Hit)		0.70	0.93 (0.17)[b]
41		0	ND[a]
45a		0.47	ND[a]

7

45b	0.88	ND[a]
45c	1.23	0.88 (0.08)[b]
45d	0.04	ND[a]
45e	0.58	ND[a]
45f	0	ND[a]

[a]ND : Not determined. [b]Standard deviation given between parentheses.

Mechanism of inhibition of mycobacterial ThyX

The inhibition profile of 5 compounds (**22a, 22c, 22e, 22i, 22k**) was probed as described in the methods section. The results were similar for all tested compounds and the data obtained for compound **22e** as a representative example are shown in Figure 4. The IC_{50} versus dUMP plot (Figure 4, insert A) suggested that a non-competitive inhibition pattern can best describe the inhibition by selected molecules against dUMP. The same set of molecules showed a competitive inhibition pattern against CH_2H_4Folate with a linear variation of IC_{50} in function of the CH_2H_4Folate concentration. An analogous plot for NADPH revealed a characteristic behavior for uncompetitive inhibition for the same set of molecules regarding NADPH binding. These results suggest that molecules could bind ThyX as a complex of type ThyX-NADPH or ThyX-NADP^{+}.

The observation that the IC_{50} values determined from the dose–response curves were of the same order of magnitude as the total enzyme concentration used suggested a tight-binding inhibition mechanism for the tested molecules, as previously described for 2-hydroxy-1,4-naphthoquinone analogues as tight binding inhibitors for *PBCV-1* ThyX.[13]

The qualitative evaluation of the ability of molecules **22a, 22c, 22e, 22i, 22k, 27, 28, 29d, 48** and **62** to inhibit ThyX from species besides *M. tuberculosis* (e.g. *H. pylori, PBCV-1, B. hermsi, C. trachomatis*) was also undertaken. None of these analogues inhibited ThyX from *PBCV-1* and *B. hermsi*, whereas a weak inhibition at 50 □□ was measured for ThyX from *H. pylori* and *C. trachomatis.* Analysis of the different ThyX protein sequences revealed, in the environment of the substrate binding pocket, some interesting differences for presumed amino acids implicated in compound binding.

Molecular Docking

Since competition assays indicated that studied compounds share their binding site with tetrahydrofolate, hit compound **10**

was docked in the binding site of this cofactor. The crystal structure of *T. maritima* ThyX in complex with FAD, dUMP and folinic acid (PDB ID: 4GTA)[23] was used as starting structure to perform an initial molecular docking experiment. The aromatic and saturated rings of the benzo[b][1,4]oxazin moiety of **10** were posed on the corresponding rings of the pterin moiety of folinic acid, while the piperazine group of compound **10** fitted the aromatic ring in the *p*-amino benzoic acid moiety of folinic acid. Overlaying the obtained complex with the crystal structure of *M. tuberculosis* ThyX in complex with FAD, 5-Br-dUMP and glycerol (PDB ID: 2AF6)[24] revealed that compound **10** is accommodated in a binding site of *M. tuberculosis* ThyX that contained two glycerol molecules in the crystal structure, occupying the binding pockets of the *N*-phenyl-carboxamide and benzo[b][1,4]oxazin moieties of compound **10**. Starting from this overlay, two complexes of *M. tuberculosis* ThyX were generated after removal of both glycerols mentioned above. More specifically, both complexes contained the original FAD and 5-Br-dUMP together with compound **10** or folinic acid for comparison purposes. After an initial minimization, both complexes were subjected to 20 ns molecular dynamics calculations using the AMBER 16.0 software package[25] as described in the experimental part.

During molecular dynamics, the benzo[b][1,4]oxazin part of compound **10** and the pterine scaffold of folinic acid remained nicely stacked to the flavine moiety of FAD cofactor in the active site. Remarkably, two interconverting binding modes were observed for the glutamate moiety in folinic acid resulting in an excessive conformational disorder, thereby explaining the absence of this moiety and some residues in this region of the crystal structure of the *T. maritima* ThyX complex. In the most abundant binding mode as seen in Molecular Dynamics simulations, the □ carboxyl group of the glutamate moiety is interacting with a conserved Arg residue thereby replacing a glycerol in the initial crystal structure (*M. tuberculosis*: Arg41 in 2AF6 *T. maritima*: Arg28 in 4GTA, *H. pylori*: Arg42 in 3AH5, Figure 6). In the same binding mode, the *N*-phenyl-carboxamide of **10** shows a stacking interaction with the side chain of His63 in *M. tuberculosis* ThyX (Figure 5).

Strikingly, the carboxamide linkers in compound **10** as well as in folinic acid are within hydrogen bonding distance with the terminal hydroxyl of Ser46 in modelled complexes. While Ser46 is conserved in *H. pylori*, it is mutated to Glu46 in ThyX homologues from *B. hermsi* and *PBCV-1* for which no inhibitory activity could be observed. To examine the effect of this mutation on the binding affinity of **10**, Ser46 was mutated *in silico* to Glu46. The results indicated that this mutation does not allow formation of a hydrogen bond with the carboxamide linker in compound **10** and impaired the stability of the loop that forms the studied binding site. Additionally, a distortion of binding mode is observed at the piperazine linker. All of these effects contributed to a reduced binding affinity of the compounds, explaining the loss of inhibitory effect on ThyX from *PBCV-1 and B. hermsi* as described above.

8
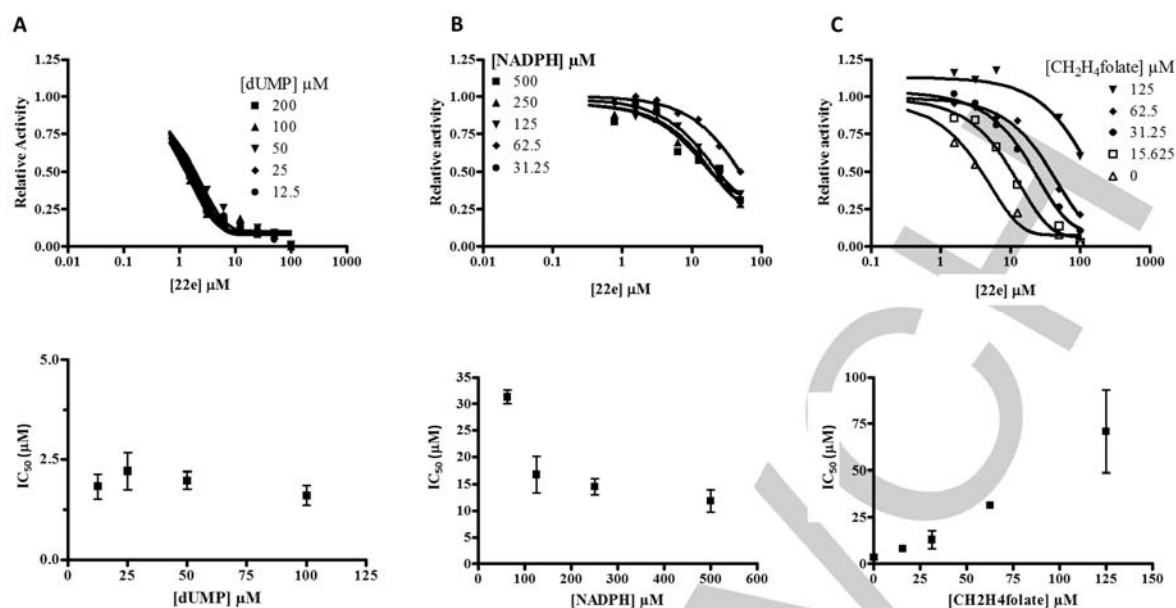
Figure 4. Secondary and final plots of results obtained with compound **22e** for mycobacterial ThyX inhibition using different concentrations of dUMP (**A**), NADPH (**B**) and methylene tetrahydrofolate (**C**).
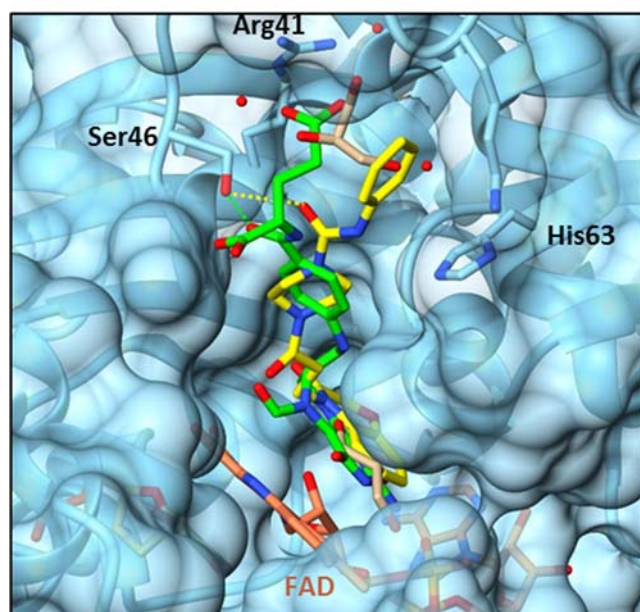
Figure 5: Compound **10** (yellow) in the catalytic site *M. tuberculosis* ThyX crystal structure (PDB ID: 2AF6) including FAD (orange) and 5-Br-dUMP. Modelled folinic acid (green) and glycerol (gold) in the binding site of the crystal structure are overlayed. Side chains of Arg41, Ser46 and His63 in subunit D are depicted. Green and yellow dashed lines indicate putative hydrogen bonds of Ser46 and the carboxamide linkers in folinic acid and compound **10**, respectively.

The model of compound **10** bound to *M. tuberculosis* ThyX enabled to rationalize the SAR results (Figure 7). The carbonyl in the benzoxazine moiety forming the δ-lactam ring accepted a hydrogen bond from Ser102, the only residue of subunit D that directly interacted with compound **10** in our model. Intermittently, the same Ser102 donated a hydrogen bond to the oxygen in the 1,4 oxazine moiety, albeit this bifurcated hydrogen bond was weaker because of the more spread-out orientation of both acceptors. The insertion of a nitrogen atom in the phenyl part of the benzo[b][1,4]oxazin moiety, yielded pyrido[3,2-b][1,4]oxazine **48**, from which the nitrogen atom acted as an isostere for O4 of the pterin ring of the original cofactor and aligns the attached oxazine and aromatic ring stronger with the heterocycle of FAD in a parallel-displaced orientation as observed for compound **10**. Additionally, the more polar character of the pyridine ring of compound **48** allowed a hydrogen bond with His69. The absence of the aforementioned heterocycles in compound **59**, together with its complete lack of ThyX inhibition, supported this interaction analysis.

The introduction of a methoxy moiety at the *para* position in **22b** during the SAR of the *N*-phenylcarboxamide moiety was expected to destabilize the flexible closing loop which contributes to the lower activity. For comparison, the *meta*-acetyl variant (compound **22g**) provides a stronger acceptor (no mesomeric effect with carboxamide) which might accept an additional hydrogen bond from Thr54 resulting in a tighter loop closing with relative inhibition of 1.06 compared to 0.70 in compound **10**. The nitrogen from the pyridine moieties in compounds **27** and **28** occupied a smaller volume compared to the acetyl group in **22b** with higher atomic radius and could act

9

FULL PAPER

Figure 6. Sequence alignment of ThyX homologues by CDD/SPARCLE.[26] Residues that are labeled in Figure 5 are boxed.

as hydrogen bond acceptor for the conserved Arg41. Such increased loop stabilization correlated with the higher relative inhibition values of 1.19 and 1.13 observed for compounds **27** and **28** respectively. The benzyl derivative **22k** covered a larger rotational space than the phenyl analogue **10,** providing increased potential stacking interactions with His63 and Tyr54. Moreover, the increased flexibility of compound **22k** resulted in a more stable stacking interaction between the benzoxazine moiety and the heterocycle of FAD, maintaining the His63 stacking interaction and Ser46 hydrogen bond.

Figure 7. LigPlot+ representation of interacting residues with native folinic acid (A), hit-compound **10** (B) and optimized compound **29d** (C)

With an additional methylene bridge adjacent to the piperazine linker in compound **29d,** an additional source of rotational freedom was introduced, similarly as for compound **22k**. A model of *M. tuberculosis* ThyX in complex with the most active ThyX inhibitor (compound **29d**) was obtained as described in the method section. The additional *N*-methyl group contributed to hydrophobic Van der Waals interactions with Tyr44, thereby positioning the phenyl ring towards optimal perpendicular stacking interaction with His63 and optimizing the geometry of hydrogen bond formation with Ser46. Because of the increased flexibility resulting from the methylene group, a bifurcated hydrogen bond formation of the carbonyl group in the *N*-phenyl carboxamide was viable with Ser46 and Tyr60 which concurrently positioned the phenyl moiety through stacking. Compared to the binding conformation of compound **10,** this overall network of stabilizing hydrophobic and increased electrostatic interactions in **29d** allowed a volumetric occupation of the binding space of the glutamate moiety in folinic acid flanked by Arg41 and His63. These results were further quantified by interaction energy calculations in which a difference of 8.69 kcal/mol was observed with a more favorable affinity for **29d** (folinic acid: -37.90 kcal/mol, compound **10**: -38.77 kcal/mol, compound **29d**: -46.59 kcal/mol). Furthermore, an overall slight rotational shift resulted in more planar stacking interaction between the benzoxazine moiety and the FAD cofactor. Finally, an additional hydrogen bond was possible between one hydroxyl from the glycerol linker in FAD and

10

the oxygen from the benzoxazine ring. The same reasoning was applied to compounds **29a** and **29c**, explaining the potent inhibitory activity of both compounds (relative inhibition at 5 µM of 0.89 and 0.99, respectively).

In compound **45c**, the exocyclic aminogroup at the piperidine moiety had a similar effect as the extra methylene in compounds **29a**, **29c** and **29d**. Alterations in the piperazine moiety, albeit with limited conformational space, displayed a positioning role for the binding mode of this central part in the entire compound. Compounds **45d** and **45f** shifted the heterocycle by one atom resulting in loss of activity and thereby endorsing the positioning function. The methyl side chain in compound **45b** resided in a more hydrophobic pocket displaying hydrophobic interactions with Val72 and Ile64 resulting in a slightly higher relative inhibition (0.88).

In the SAR of the propanoyl linker (compounds **32**, **33**, **36**, **37** and **39**), the loss of inhibitory activity by shortening the linkers provided evidence for the necessary co-occurrence of both His63 stacking and Ser46 and Tyr60 bifurcated hydrogen bond interactions with benzoxazine alignment to the FAD heterocycle.

Conclusions

Starting from the previously identified hit compound **10**, a hit-to-lead optimization campaign was performed in order to discover novel mycobacterial ThyX inhibitors. The most potent analogue of this series was endowed with an IC_{50} of 0.69 µM against mycobacterial ThyX. Molecular modeling was applied in order to understand the SAR for *M. tuberculosis* ThyX and the variation in activity towards ThyX from other microorganisms. These results open new avenues for structure-based drug design to discover more potent ThyX inhibitors with antibacterial activity. A phenotypic screening for antimicrobial activity of the most potent molecules on specific bacteria will be the first step to address the path forward of these compounds.

Experimental Section

General

All reagents and solvents were purchased from commercial sources and used as obtained. Moisture sensitive reactions were carried out using oven-dried glassware under a nitrogen or argon atmosphere. ^1H and ^{13}C NMR spectra were recorded on a Bruker Avance 300 or 500 MHz spectrometer with tetramethylsilane as internal standard or referenced to the residual solvent signal. The following abbreviations were used to explain multiplicities: s = singlet, d = doublet, t = triplet, q = quartet, m = multiplet, br = broad, dd = doublet of doublets. Coupling constants are expressed in Hz. High-resolution mass spectra (HRMS) were obtained on a quadruple orthogonal acceleration time-of-flight mass spectrometer (Synapt G2 HDMS, Waters, Milford, MA). Samples were infused at 3 µL/min, and spectra were obtained in positive (or negative) ionization mode with a resolution of 15 000 (fwhm) using leucine enkephalin as the lock mass. Pre-coated aluminum sheets (254 nm) were used for TLC and spots were visualized with UV light. The products were purified by flash column chromatography on silica gel (60 Å, 0.035−0.070 mm, Acros Organics). The purity of final compounds was determined by analytical RP-HPLC, using one of the following methods. Method A: a Waters 600 HPLC system and a Waters 2996 photodiode array detector, XBridge column (C-18, 5 µm, 4.6 mm × 150 mm). Elution with a gradient mixture of H_2O containing 0.2% (vol) of TFA (A) and acetonitrile (B). Method B: a

Shimadzu HPLC equipped with a LC-20AT pump, DGU-20A5 degasser, and a SPD20A UV−VIS detector; Symmetry C18 column (5 µm, 4.6 mm × 150 mm); gradient elution of H_2O/CH_3CN from 95/5 or 70/30 to 5/95 over 25 min; flow rate 1 mL/min; wavelength, UV 254 nm. Compounds that were submitted for biological testing displayed a purity of 95% or more.

N-Phenylpiperazine-1-carboxamide (16)

To a solution of *N*-Boc piperazine **14** (0.50 mmol) in THF (10 ml) was added slowly a solution of phenyl isocyanate (0.57 mmol) in THF (10 ml) at room temperature. After the reaction reached completion, trifluoroacetic acid (10 ml) was added dropwise while stirring at 0°C. When TLC showed complete deprotection, water (100 ml) was added. The mixture was extracted with dichloromethane (30 ml). The pH of the aqueous phase was adjusted to 9 with 1N NaOH and then extracted with dichloromethane (100 ml). The organic phase was dried over Na_2SO_4. The solvents were evaporated *in vacuo* yielding a crude residue, which was used as such for further reaction without any additional purification. ^1H-NMR (300 MHz, DMSO-d_6): δ = 2.7 (brs, 2H, CH_2), 3.34 (t, *J* = 4.35 Hz, 4H, 2CH_2), 4.22 (brs, 2H, CH_2), 6.93 (t, *J* = 7.2 Hz, H, CH), 7.33 (t, *J* = 7.55 Hz, 2H, 2CH), 7.45 (d, *J* = 7.8 Hz, 2H, 2CH), 8.53 (s, H, CH) ppm. ^{13}C-NMR (75 MHz, DMSO-d_6): δ = 31.68, 36.66, 67.17, 115.35, 116.77, 122.93, 123.68, 128.31, 145.07, 164.13, 172.35 ppm.

4-(3-(6-Chloro-3-oxo-2H-benzo[b][1,4]oxazin-4(3H)-yl)propanoyl)-*N*-phenylpiperazine-1-carboxamide (17a)

A mixture of 6-chloro-2H-benzo[b][1,4]oxazin-3(4H)-one (91 mg 0.5 mmol), K_2CO_3 (158 mg, 1 mmol) and ethyl 3-bromopropionate (91 mg, 0.51 mmol) in DMF (15 ml), was stirred at 80 °C for 8 hours. Then, the mixture was diluted with water (45 ml) and extracted with dichloromethane (100 ml). The organic layer was separated, washed with water (20 ml) and dried over anhydrous Na_2SO_4. The solvents were removed under reduced pressure. The crude residue was dissolved in THF (10 ml) and a solution of LiOH (210 mg 5 mmol) in water (10 ml) was added. The reaction mixture was stirred at 60 °C for 12 hours. After the reaction reached completion, the pH was adjusted to 3 by the addition of a 2N hydrochloric acid solution. The mixture was extracted with ethyl acetate (5 x 20 ml) and dried over anhydrous Na_2SO_4. Evaporation of the solvent yielded the carboxylic acid **13a**. The compound was redissolved in DMSO (10 ml). *N*-Phenylpiperazine-1-carboxamide **16** (102 mg 0.50 mmol), HCTU (206 mg, 0.50 mmol) and DIPEA (50 µl) were added. The reaction mixture was stirred overnight at room temperature. The reaction mixture was diluted with dichloromethane (100 ml) and washed with water (40 mL), dried over Na_2SO_4, concentrated and purified by flash column chromatography to afford the title compound (318 mg, 72 %). Purity (Method A): 95.86 %. ^1H-NMR (300 MHz, CDCl$_3$): δ = 2.75 (t, *J* = 7.6 Hz, 2H, CH_2), 3.50-3.57 (m, 6H, 6CH), 3.75 (t, *J* = 7.5 Hz, 2H, CH_2), 4.25 (t, *J* = 7.8 Hz, 2H, CH_2), 4.60 (s, 2H, CH_2), 6.75 (s, H, NH), 6.94-7.10 (m, 4H, CH), 7.31-7.37 (m, 4H, 4CH) ppm. ^{13}C-NMR (75 MHz, CDCl$_3$): δ = 30.69, 38.26, 41.21, 44.15, 45.27, 68.18, 108.06, 115.08, 118.42, 120.45, 123.77, 124.00, 129.13, 138.90, 140.06, 144.24, 155.60, 164.64, 169.28 ppm. HRMS (ESI): m/z [M+H]$^+$ calculated for $C_{22}H_{24}N_4O_4Cl$ 443.14859, found 443.1476.

Compounds **17b-h** were synthesized according to the procedure for the preparation of compound **17a**. Exact experimental and spectral data can be found in the Supporting Information.

Ethyl 3-(3-oxo-2,3-dihydro-4H-benzo[b][1,4]oxazin-4-yl)propanoate (19)

A solution of **18** (2.98 g, 20 mmol) and K_2CO_3 (40 mmol, 5.52 g) in DMF (45 ml) was stirred at room temperature for 15 minutes. Then, ethyl 3-bromopropionate (22 mmol, 3.98 g) was added and the mixture was stirred overnight at 90°C. The precipitate was filtered off and the filtrate was evaporated *in vacuo*. The crude residue was purified by silica gel flash chromatography (the mobile phase being a mixture of heptane and ethylacetate in a ratio of 7:3) affording the title compound as a colorless oil

11

(4.7 g, 95 %). ^{1}H-NMR (300 MHz, CDCl$_3$): δ = 7.1 – 6.95 (m, 4H), 4.58 (s, 2H, O-CH$_2$-CO), 4.23 (t, 2H, J = 7.5 Hz, NCH$_2$), 4.13 (q, 2H, J = 7.1 Hz, CO-CH$_2$), 2.68 (t, 2H, J = 7.7 Hz, N-CH$_2$-C**H$_2$**), 1.23 ppm (t, 3H, J = 7.1 Hz, CH$_3$). ^{13}C-NMR (75 MHz, CDCl$_3$): δ = 171.1, 164.5, 145.5, 128.3, 124.2, 123.0, 117.4, 114.7, 67.7, 61.0, 37.2, 32.1, 14.2 ppm. HRMS (ESI): m/z [M+H]$^+$ calculated for C$_{13}$H$_{16}$NO$_4$ 250.10737, found 250.1071.

3-(3-Oxo-2,3-dihydro-4H-benzo[b][1,4]oxazin-4-yl)propanoic acid (20)

To a solution of **19** (4.88 g, 19.58 mmol) in THF (70 ml) was added a solution of LiOH (4.93 g, 117.46 mmol) in water (50 ml). The reaction mixture was stirred overnight at 45°C. The reaction was quenched by the addition of a 5M HCl solution (24 ml). The organic solvents of the reaction mixture were evaporated and a precipitate was formed. The precipitate was filtered off and dried yielding the title compound as a white-brown powder (3.96 g, 92 %). ^{1}H-NMR (300 MHz, DMSO-d$_6$): δ = 12.39 (s, 1H, OH), 7.24-7.15 (m, 1H), 7.10 – 6.95 (m, 1H), 4.61 (s, 2H, O-CH$_2$-CO), 4.11 (t, 2H, J = 7.6 Hz, NCH$_2$), 2.53 ppm (t, 2H, J = 7.5 Hz, N-CH$_2$-CH$_2$). ^{13}C-NMR (75 MHz, DMSO-d$_6$): δ = 172.2, 164.0, 144.9, 128.2, 123.5, 122.8, 116.6, 115.2, 67.0, 36.5, 31.5 ppm. HRMS (ESI): m/z [M-H]$^-$ calculated for C$_{11}$H$_{10}$NO$_4$ 220.06152, found 220.0637.

4-(3-Oxo-3-(piperazin-1-yl)propyl)-2H-benzo[b][1,4]oxazin-3(4H)-on (21)

A solution of **20** (1.00 g, 4.52 mmol), HOBt (0.692 g, 4.52 mmol) and DCC (1.12 g, 5.42 mmol) in DMF (16 ml) was stirred for 2 hours at room temperature. The reaction mixture was cooled down to room temperature and piperazine (0.779 g, 9.04 mmol) was added. The reaction was stirred overnight at room temperature. The precipitate was filtered off and the filtrate was evaporated *in vacuo*. The crude residue was purified by silica gel flash chromatography (mobile phase being a mixture of CH$_2$Cl$_2$:CH$_3$OH:NH$_{3(aq)}$ in a ratio of 98:2:0.3), yielding the title compound as a light yellow oil (0.4 g, 31 %). ^{1}H-NMR (300 MHz, CDCl$_3$): δ = 7.15-6.95 (m, 4H), 4.57 (s, 2H, O-CH$_2$-CO), 4.24 (t, 2H, J = 7.8 Hz, N-**CH$_2$**-CH$_2$-CO), 3.60 – 3.37 (m, 4H), 2.90-2.78 (m, 4H), 2.69 (t, 2H, J = 7.8, N-CH$_2$-C**H$_2$**-CO), 2.50 (br s, 1H), 1.23 (s, 1H, NH) ppm. ^{13}C-NMR (75 MHz, CDCl$_3$): δ = 168.8, 164.6, 145.4, 128.3, 124.2, 123.2, 117.3, 115.0, 67.7, 46.7, 46.2, 45.8, 42.6, 40.9, 38.2, 30.7, 29.8 ppm. HRMS (ESI): m/z [M+H]$^+$ calculated for C$_{15}$H$_{20}$N$_3$O$_3$ 290.14990, found 290.1505.

N-(3-Chlorophenyl)-4-(3-(3-oxo-2,3-dihydro-4H-benzo[b][1,4]oxazin-4-yl)propanoyl)piperazine-1-carboxamide (22a)

To a solution of compound **21** (89.7 mg, 0.31 mmol) in DMF (2 ml) was added 3-chlorophenyl isocyanate (71.4 mg, 0.47 mmol) and the resulting mixture was stirred overnight at room temperature. Reaction completion was monitored by TLC (CH$_2$Cl$_2$:MeOH:NH$_{3(aq)}$ 90:10:0.3). The solvents were evaporated *in vacuo* and the crude residue was purified by silica gel column chromatography (ethyl acetate 100% as mobile phase) affording the title compound as a white solid (100 mg, 73 %). Purity (Method A): 99.83 %. ^{1}H-NMR (300 MHz, CDCl$_3$): δ = 7.40 (s, 1H), 7.30-6.93 (m, 8H), 4.57 (s, 2H, O-CH$_2$-CO), 4.25 (t, 2H, J = 7.6 Hz, N-CH$_2$-CH$_2$-CO), 3.70-3.60 (m, 2H), 3.58-3.38 (m, 6H), 2.71 (t, 2H, J = 7.9 Hz, N-CH$_2$-CH$_2$-CO) ppm. ^{13}C NMR (75 MHz, CDCl$_3$): δ = 169.1, 164.7, 154.8, 145.4, 140.3, 134.4, 129.9, 128.2, 124.4, 123.4, 120.3, 118.3, 117.4, 114.8, 67.7, 45.2, 44.0, 43.7, 41.2, 37.9, 30.8 ppm. HRMS (ESI): m/z [M+H]$^+$ calculated for C$_{22}$H$_{24}$ClN$_4$O$_4$ 443.14804, found 443.1486.

Compounds **22b-n** were synthesized according to the procedure for the preparation of compound **22a**. Exact experimental and spectral data can be found in the Supporting Information.

4-(3-(3-Oxo-2,3-dihydro-4H-benzo[b][1,4]oxazin-4-yl)propanoyl)-*N*-(pyridin-4-yl)piperazine-1-carboxamide (27)

To a solution of 4-aminopyridine **23** (24.67 mg, 0.262 mmol), DIPEA (42.3 mg, 0.328 mmol) in DMF (1 ml) was added phenyl chloroformate (44.5 mg, 0.284 mmol) at 0 °C. The mixture was stirred for 15 minutes and completion of the reaction was monitored by TLC (CH$_2$Cl$_2$:CH$_3$OH:NH$_{3(aq)}$, 92:8:0.3). DIPEA (42.3 mg, 0.328 mmol) and a solution of compound **21** (63.2 mg, 0.218 mmol) in DMF (1 ml) were added. The resulting reaction mixture was stirred overnight at room temperature. The solvents were evaporated *in vacuo*. The residue was dissolved in ethyl acetate and washed with water. The organic phase was dried over Na$_2$SO$_4$, and concentrated *in vacuo*. The crude residue was purified by silica gel column chromatography (using a mixture of dichloromethane and methanol as mobile phase, in a gradient gradually increasing from 5 to 10% methanol) affording the title compound as an off-white solid (28 mg, 32 %). Purity (Method A): 100 %. ^{1}H-NMR (300 MHz, CDCl$_3$): δ 8.38-8.32 (m, 2H), 7.93 (br s, 1H), 7.42-7.35 (m, 2H), 7.10-6.95 (m, 4H), 4.57 (s, 2H, O-CH$_2$-CO), 4.24 (t, 2H, J = 7.6 Hz, N-CH$_2$-CH$_2$-CO), 3.70-3.42 (m, 8H), 2.71 (t, 2H, J = 7.8 Hz, N-CH$_2$-CH$_2$-CO) ppm. ^{13}C-NMR (75 MHz, CDCl$_3$): δ 169.1, 164.8, 154.2, 150.1 (2C), 147.1, 145.4, 128.2, 124.4, 123.2, 117.5, 114.8, 113.7 (2C), 67.7, 45.3, 44.2, 43.8, 41.2, 38.0, 30.9 ppm. HRMS (ESI): m/z [M+H]$^+$ calculated for C$_{21}$H$_{24}$N$_5$O$_4$ 410.18226, found 410.1817.

Compound **28** was synthesized according to the procedure for the preparation of compound **27**. Exact experimental and spectral data can be found in the Supporting Information.

2-(4-(3-(3-Oxo-2H-benzo[b][1,4]oxazin-4(3H)-yl)propanoyl)piperazin-1-yl)-*N*-(pyridin-3-yl)acetamide (29a)

To a solution of 2-(piperazin-1-yl)-*N*-(pyridin-3-yl)acetamide (110 mg, 0.5 mmol) in DMSO (10 ml) was added compound **20** (110 mg 0.50 mmol), HCTU (206 mg 0.5 mmol) and DIPEA (50 µl). The reaction mixture was stirred overnight at room temperature. Then, the mixture was diluted with CH$_2$Cl$_2$ (100 ml) and washed with water (40 ml). The combined organic layers were dried over Na$_2$SO$_4$ and concentrated *in vacuo*. The crude residue was purified by silica gel flash column chromatography affording the title compound (171 mg, 81 %). Purity (Method A): 100 %. ^{1}H-NMR (300 MHz, CDCl$_3$): δ = 2.60-2.62 (m, 4H, 2CH$_2$), 2.73 (t, J = 7.8 Hz, 2H, CH$_2$), 3.19 (s, 2H, CH$_2$), 3.56-3.58 (m, 2H, CH$_2$), 3.71-3.72 (m, 2H, CH$_2$), 4.28 (t, J = 7.65 Hz, 2H, CH$_2$), 4.59 (s, H, CH$_2$), 7.01-7.12 (m, 4H, 4CH), 7.27-7.31(m, 1H, 1CH), 8.19-8.23 (m, 1H, 1CH), 8.32-8.37 (m, 1H, 1CH), 8.59 (d, J = 2.4 Hz, H, CH), 9.05 (m, H, NH), ppm. ^{13}C-NMR (75 MHz, CDCl$_3$): δ = 30.74, 38.05, 41.62, 45.53, 53.20, 53.55, 61.92, 67.66, 114.86, 117.35, 123.16, 124.26, 126.92, 128.24, 134.22, 124.11, 141.01, 145.58, 164.63, 168.32, 168.87 ppm. HRMS (ESI): m/z [M+H]$^+$ calculated for C$_{22}$H$_{26}$N$_5$O$_4$ 424.19846, found 424.1976.

Compounds **29b-d** synthesized according to the procedure for the preparation of compound **29a**. Exact experimental and spectral data can be found in the Supporting Information.

Ethyl 2-(3-oxo-2,3-dihydro-4H-benzo[b][1,4]oxazin-4-yl)acetate (30)

1,4-Benzoxazin-3(4*H*)-one **18** (5.00 g, 33.52 mmol) and K$_2$CO$_3$ (13.90 g, 100.57 mmol) were dissolved in DMF (80 ml) and stirred at room temperature for 15 minutes. Then, ethyl bromoacetate (11.20 g, 67 mmol) was added and the reaction mixture was stirred overnight at 90 °C. The solvents were evaporated *in vacuo* and the residue was purified by silica gel column chromatography (using a mixture of cyclohexane and ethyl acetate in a ratio of 7:3 as mobile phase) affording the title compound as a colorless oil (7.70 g, 98 %). ^{1}H-NMR (300 MHz, CDCl$_3$): δ = 7.05-6.94 (m, 3H), 6.78-6.70 (m, 1H), 4.65 (s, 2H), 4.63 (s, 2H), 4.22 (q, 2H, J = 7.14 Hz), 1.26 (t, 3H, J = 7.12 Hz) ppm. ^{13}C-NMR (75 MHz, CDCl$_3$): δ = 167.8, 164.9, 145.1, 128.7, 124.3, 123.0, 117.2, 114.5, 67.5, 61.9, 43.0, 14.2 ppm. HRMS (ESI): m/z [M+Na]$^+$ calculated for C$_{12}$H$_{13}$N$_1$O$_4$Na 258.07370, found 258.0749.

FULL PAPER

2-(3-Oxo-2,3-dihydro-4H-benzo[b][1,4]oxazin-4-yl)acetic acid (30')

To a solution of **30** (7.70 g, 32.73 mmol) in THF (80 ml) was added a solution of LiOH (8.24 g, 196.4 mmol) in H_2O (70 ml). The resulting reaction mixture was stirred overnight at 45 °C. After completion of the reaction, the reaction mixture was acidified by addition of an excess of HCl. The organic solvent (THF) was evaporated *in vacuo* resulting in the formation of a precipitate in water. The precipitate was filtered off, washed with cold H_2O and dried furnishing the title compound as an off-white powder (6.24 g, 92 %). ^{1}H-NMR (300 MHz, DMSO): δ = 13.09 (br s, 1H), 7.10-6.95 (m, 4H), 4.69 (s, 2H), 4.63 (s, 2H) ppm. ^{13}C-NMR (75 MHz, DMSO): δ = 169.3, 164.5, 144.6, 128.7, 123.7, 122.7, 116.6, 115.3, 66.9, 42.4 ppm. HRMS (ESI): m/z [M-H]- calculated for $C_{10}H_8N_1O_4$ 206.04587, found 206.0464.

4-(2-Oxo-2-(piperazin-1-yl)ethyl)-2H-benzo[b][1,4]oxazin-3(4H)-one (30'')

2-(3-Oxo-2,3-dihydro-4H-benzo[b][1,4]oxazin-4-yl)acetic acid (1.5 g, 7.24 mmol), HOBt.H_2O (1.11 g, 7.24 mmol) and DCC (1.49 g, 7.24 mmol) were dissolved in DMF (25 ml). The mixture was stirred for 2 hours at 0°C. After the addition of piperazine (1.25 g, 14.48 mmol), the reaction was stirred overnight at room temperature. The formed precipitate was filtered off and discarded. The filtrate was concentrated *in vacuo* and the residue was purified by silica gel column chromatography (CH_2Cl_2:CH_3OH:$NH_{3(aq)}$, 92:8:0.3) yielding the title compound as a white powder (742 mg, 37 %). ^{1}H-NMR (300 MHz, DMSO): δ = 7.07- 6.98 (m, 3H), 6.93-6.88 (m, 1H), 4.78 (s, 2H), 4.66 (s, 2H), 3.53-3.47 (m, 2H), 3.42-3.36 (m, 2H), 2.84-2.77 (m, 2H), 2.73-2.66 (m, 2H) ppm. ^{13}C-NMR (75 MHz, DMSO): δ = 164.4, 164.2, 144.6, 129.1, 123.4, 122.6, 116.4, 115.6, 66.9, 45.6, 45.2, 45.1, 42.4, 42.3 ppm. HRMS (ESI): m/z [M+H]+ calculated for $C_{14}H_{18}N_3O_3$ 276.13425, found 276.1350.

4-(2-(3-Oxo-2,3-dihydro-4H-benzo[b][1,4]oxazin-4-yl)acetyl)-*N*-phenylpiperazine-1-carboxamide (32)

Compound **32** was synthesized according to the procedure described for the synthesis of compound **22a**, affording the title compound as a white powder (89 mg, 89 %). Purity (Method A): 98.76 %. ^{1}H-NMR (300 MHz, CDCl3): δ = 7.40-7.25 (m, 3H), 7.10-6.95 (m, 4H), 6.82-6.75 (m, 1H), 6.57 (br s, 1H), 4.72 (s, 2H), 4.67 (s, 2H), 3.75-3.60 (m, 6H), 3.55-3.43 (m, 2H), 1.64 (br s, 1H) ppm. ^{13}C-NMR (75 MHz, CDCl3): δ = 165.4, 165.2, 155.1, 145.3, 138.7, 129.13 (2C), 129.08, 124.4, 123.7, 123.1, 120.3 (2C), 117.3, 115.0, 67.7, 44.9, 44.3, 43.5, 43.2, 41.8 ppm. HRMS (ESI): m/z [M+H]+ calculated for $C_{21}H_{23}N_4O_4$ 395.17136, found: 395.1708.

Compounds **33, 36** and **37** were synthesized according to the procedure for the preparation of compound **32**. Exact experimental and spectral data can be found in the Supporting Information.

4-(3-(3-Oxo-2,3-dihydro-4*H*-benzo[*b*][1,4]oxazin-4-yl)propyl)-*N*-phenylpiperazine-1-carboxamide (39)

A mixture of 2*H*-benzo[*b*][1,4]oxazin-3(4*H*)-one **18** (75 mg, 0.5 mmol), K_2CO_3 (158 mg, 1.0 mmol) and *tert*-butyl 4-(3-bromopropyl)piperazine-1-carboxylate (169 mg, 0.55 mmol) in DMF (5 ml) was stirred at 65°C for 18 hours. When the reaction was finished, the mixture was diluted with water (15 ml) and extracted with dichloromethane (3x10 ml). The organic phases were combined, washed with water (15 ml), dried over anhydrous Na_2SO_4 and evaporated. The crude residue was dissolved in a 80 % TFA solution (5 ml). The mixture was stirred for 4 hours. After evaporation of the solvents, the crude residue was dissolved in THF (5 ml) and phenylisocyanate (66 mg, 0.55 mmol) was added. The mixture was stirred at room temperature overnight. The resulting mixture was diluted with CH_2Cl_2 (20 ml) and washed with water (2×20 ml). The combined organic layers were dried over anhydrous Na_2SO_4 and concentrated under reduced pressure. The residue was purified by silica gel flash column chromatography (Et_2O:MeOH 10:1) to afford the product (101 mg, 51 %).

Purity (Method A): 98.85 %. ^{1}H-NMR (300 MHz, CDCl3): δ = 1.86 (p, *J* = 7.0 Hz, 2H, CH_2), 2.42-2.47 (m, 6H, 3xCH_2), 3.47-3.51 (m, 4H, 2xCH_2), 4.02 (d, *J* = 7.0 Hz, 2H, CH_2), 4.59 (s, 2H, CH_2), 6.52 (s, 1H, NH), 6.98-7.10 (m, 5H, 4xCH_{Ar}), 7.24-7.30 (m, 2H, 2xCH_{Ar}), 7.33-7.37 (m, 2H, 2xCH_{Ar}) ppm. ^{13}C-NMR (75 MHz, CDCl3): δ = 24.41, 39.46, 41.21, 52.94, 55.50, 67.75, 114.99, 117.32, 120.09, 122.85, 123.21, 123.99, 128.64, 128.97, 139.13, 145.52, 155.15, 164.43 ppm.

4-(3-(1,4-Diazepan-1-yl)-3-oxopropyl)-2H-benzo[b][1,4]oxazin-3(4H)-on (40)

A solution of compound **20** (0.800 g, 3.62 mmol), HOBt (0.554 g, 3.62 mmol) and DCC (0.746 mg, 3.62 mmol) in DMF (12 ml) was stirred at room temperature for 2 hours. Then, the mixture was cooled down to 0°C and homopiperazine (0.725 g, 7.23 mmol) was added. The reaction mixture was stirred overnight at room temperature. The precipitate was filtered off and washed with dichloromethane. The filtrate was evaporated and the residue was purified by silica gel flash chromatography (the mobile phase being CH_2Cl_2:MeOH:NH_3(aq) 92:8:0.3), yielding the title compound as a light yellow oil (0.506 g, 46 %). ^{1}H-NMR (300 MHz, CDCl3): δ = 7.10 – 7.02 (m, 1H), 6.98 – 6.87 (m, 3H), 4.49 (s, 2H, O-CH_2-CO), 4.19 (t, 2H, *J* = 7.7 Hz, N-CH_2-CH_2-CO), 3.60-3.50 (m, 2H), 3.48-3.35 (m, 2H), 2.88 - 2.82 (m, 2H), 2.79 – 2.71 (m, 2H), 2.69 – 2.56 (m, 2H), 1.85 (s, 1H, NH), 1.75 – 1.65 (m, 2H) ppm. ^{13}C-NMR (75 MHz, CDCl3): δ = 169.7, 164.3, 145.1, 128.2, 123.9, 123.0, 117.0, 114.8, 67.5, 50.7, 48.6, 44.5, 38.0, 30.7, 30.4, 29.4 ppm. HRMS (ESI): m/z [M+H]+ calculated for $C_{16}H_{21}N_3O_3$ 304.16555, found 304.1655.

4-(3-(3-Oxo-2,3-dihydro-4H-benzo[b][1,4]oxazin-4-yl)propanoyl)-*N*-phenyl-1,4-diazepane-1-carboxamide (41)

This compound was synthesized from compound **40**, according to the procedure for the synthesis of compound **22a**. The crude residue was purified by silica gel flash chromatography (using ethyl acetate as mobile phase), yielding the title compound as a white powder (93 % yield). Purity (Method A): 100 %. ^{1}H-NMR (300 MHz, CDCl3): δ 7.40 - 7.34 (m, 4H), 7.10 – 6.95 (m, 5H), 6.72 – 6.69 (m, 1H), 4.57 (s, 2H, O-CH_2-CO), 4.29 - 4.15 (m, 2H, N-CH_2-CH_2-CO), 3.77 - 3.68 (m, 1H), 3.65 – 3.53 (m, 5H), 3.50 – 3.40 (m, 2H), 2.75 – 2.65 (m, 2H, *J* = 7.2 Hz, N-CH_2-CH_2-CO), 1.98 (m, 2H) ppm. HRMS (ESI): m/z [M+H]+ calculated for $C_{23}H_{26}N_4O_4$ 423.20266, found 423.2027.

(*S*)-2-Methyl-4-(3-(3-oxo-2H-benzo[b][1,4]oxazin-4(3H)-yl)propanoyl)-*N*-phenylpiperazine-1-carboxamide (45a)

(*S*)-*tert*-Butyl 3-methylpiperazine-1-carboxylate **42a** (100 mg 0.50 mmol) was dissolved in THF (10 mL) and a solution of phenylisocyanate (60 mg 0.57 mmol) in THF (5 mL) was slowly added at room temperature. A light yellow solid was formed upon reaction completion. Then, trifluoroacetic acid (10 ml) was added dropwise while stirring at 0°C. When TLC showed completion of the deprotection, the mixture was diluted with water (50 ml). Then, the mixture was washed with dichloromethane (30 ml) and the pH of the aqueous phase was adjusted to 9 by the addition of 1N NaOH. The mixture was extracted with dichloromethane (50 ml). The combined organic layers were dried over Na_2SO_4. The solvents were evaporated *in vacuo*, affording crude **44a**. This solid was used in the next reaction without further purification. The solid was redissolved in DMSO (10 ml). Compound **20** (110 mg, 0.50 mmol), HCTU (206 mg 0.50 mmol) and DIPEA (50 µl) were added. The mixture was stirred overnight at room temperature. The resulting mixture was diluted with CH_2Cl_2 (100 ml) and washed with water (40 ml). The combined organic layers were dried over Na_2SO_4 and concentrated *in vacuo*. The crude residue was purified by silica gel flash column chromatography yielding the title compound (210 mg, 50 %). Purity (Method A): 98.77 %. ^{1}H-NMR (300 MHz, DMSO-d6): δ = 1.05-1.19 (m, 3H, CH_3), 2.67-3.14 (m, 5H, CH_2, CH), 3.65-4.38 (m, 6H, 3CH_2), 4.63 (s, 2H, CH_2), 6.94-7.08 (m, 1H, CH), 7.20-7.25 (m, 3H, 3CH), 7.43-7.48 (m, 3H, 3CH), 8.54 (s, H, NH) ppm. ^{13}C-NMR (75 MHz, DMSO-d6): δ =14.71, 15.24, 29.82, 33.08, 37.33, 47.21, 43.80, 44.81, 45.08, 46.51, 48.94, 67.21,

13

115.32, 115.45, 116.77, 119.95, 121.97, 123.02, 123.69, 128.41, 140.54, 145.04, 154.91, 161.16, 169.20, 169.30 ppm. HRMS (ESI): m/z [M+H]$^+$ calculated for $C_{23}H_{27}N_4O_4$ 423.20321, found 423.2025.

Compounds **45b-f** were synthesized according to the procedure for the preparation of compound **45a**. Exact experimental and spectral data can be found in the Supporting Information.

4-(3-(3-Oxo-2,3-dihydro-4*H*-pyrido[3,2-*b*][1,4]oxazin-4-yl)propanoyl)-*N*-phenylpiperazine-1-carboxamide (48)

A mixture of 2*H*-pyrido[3,2-*b*][1,4]oxazin-3(4*H*)-one **46** (75 mg, 0.5 mmol), K_2CO_3 (158 mg, 1.0 mmol), DMF (3 ml), and ethyl 3-bromopropionate (100 mg, 0.55 mmol) was stirred at 80°C for 8 hours. When the reaction was finished, the mixture was diluted with water (15 ml) and extracted with dichloromethane (3x10 ml). The combined organic phases were washed with water (15 ml) dried over anhydrous Na_2SO_4 and evaporated *in vacuo*. The crude residue was dissolved in THF (5 ml) and a solution of LiOH (42 mg, 1 mmol) in H_2O (5 ml) was added. The mixture was stirred for 18 hours at 60°C. Then, the pH was adjusted to 3 with 2N hydrochloric acid and the compound was extracted with ethyl acetate (3x20 ml). The combined organic layers were dried over anhydrous Na_2SO_4. The solvents were evaporated *in vacuo*, yielding the pure carboxylic acid compound. The acid was redissolved in DMF (5 ml), and HOBt (76 mg, 0.5 mmol) and DCC (103 mg, 0.5 mmol) were added at 0°C. After stirring for two hours, *N*-phenylpiperazine-1-carboxamide **16** (102 mg, 0.5 mmol) was added. The mixture was stirred at room temperature overnight. The resulting mixture was diluted with CH_2Cl_2 (20 ml) and washed with water (2×20 ml). The organic phases were dried over anhydrous Na_2SO_4, and concentrated *in vacuo*. The crude residue was purified by flash column chromatography (using a mixture of diethylether and methanol in a ratio of 10:1 as mobile phase) to afford the title compound (135 mg, 66 %). Purity (Method A): 100 %. ^{1}H-NMR (300 MHz, CDCl$_3$): δ = 2.76-2.81 (m, 2H, CH$_2$), 3.46-3.69 (m, 8H, 4xCH$_2$), 4.42-4.47 (m, 2H, CH$_2$), 4.66 (s, 2H, CH$_2$), 6.62 (s, 1H, NH), 6.94 (dd, *J* = 7.9, 4.9 Hz, 1H, CH$_{Ar}$), 7.01-7.07 (m, 1H, CH$_{Ar}$), 7.23 (dd, *J* = 7.9, 1.5 Hz, 1H, CH$_{Ar}$), 7.27 – 7.38 (m, 4H, CH$_{Ar}$), 8.00 (dd, *J* = 4.9, 1.5 Hz, 1H, CH$_{Ar}$) ppm. ^{13}C-NMR (75 MHz, CDCl$_3$): δ = 31.49, 36.41, 41.12, 43.62, 44.19, 45.33, 67.50, 119.54, 120.35, 123.51, 123.66, 129.01, 138.89, 140.74, 141.34, 141.45, 155.18, 164.88, 169.49 ppm. HRMS (ESI): m/z [M+H]$^+$ calculated for $C_{21}H_{24}N_5O_4$ 410.18228, found 410.1818.

Compounds **49, 53-55, 58-59** were synthesized according to the procedure for the preparation of compound **48**. Exact experimental and spectral data can be found in the Supporting Information.

4-(3-(2-Oxoquinoxalin-1(2H)-yl)propanoyl)-*N*-phenylpiperazine-1-carboxamide (62)

A mixture of *tert*-butyl 3-oxo-3,4-dihydroquinoxaline-1(2*H*)-carboxylate **60** (248 mg, 1 mmol), K_2CO_3 (276 mg, 2.0 mmol) and ethyl 3-bromopropionate (199 mg, 1.1 mmol) in DMF (6 ml) was stirred at 80°C for 8 hours. When the reaction was finished, the mixture was diluted with water (30 ml) and extracted with dichloromethane (3x15 ml). The organic phases were combined and washed with water (30 ml). The combined organic phases were dried over anhydrous Na_2SO_4 and evaporated *in vacuo*. The crude residue was redissolved in THF (10 ml) and a solution of LiOH (84 mg, 2 mmol) in H_2O (10 ml) was added. The mixture was stirred for 18 hours at 60°C. Then, the pH was adjusted to 3 with 2N hydrochloric acid and the compound was extracted with ethyl acetate (3x20 ml). The combined organic layers were dried over anhydrous Na_2SO_4 and evaporated *in vacuo*, yielding the pure acid. The acid was dissolved in DMF (10 ml), and HOBt (153 mg, 1 mmol), DCC (206 mg, 1 mmol) were added at 0°C. After stirring for 2 hours, *N*-phenylpiperazine-1-carboxamide **16** (204 mg, 1 mmol) was added and the mixture was stirred overnight at room temperature. The resulting mixture was diluted with CH_2Cl_2 (30 ml) and washed with water (2×20 ml). The combined organic layers were dried over anhydrous Na_2SO_4 and concentrated *in vacuo*. The crude residue was purified by flash column chromatography (Et$_2$O:MeOH 10:1) affording

compound **61**. *N*-Boc deprotection was carried out by using a 3 ml 80 % TFA in 15 ml of CH_2Cl_2. After stirring for 3 hours at 0°C, solvents were evaporated and the crude mixture was dissolved in CH_2Cl_2 (20 ml), washed with a saturated aqueous NaHCO$_3$ solution. The combined organic layers were dried over anhydrous Na_2SO_4, concentrated and purified by flash column chromatography (EtOAc:MeOH 10:1) yielding the title compound (102 mg, 25 %). Purity (Method A): 98.86 %. ^{1}H-NMR (300 MHz, CDCl$_3$): δ = 2.77-2.85 (m, 2H, CH$_2$), 3.47-3.50 (m, 4H, 2xCH$_2$), 3.51 (s, 2H, CH$_2$), 3.69-3.73 (m, 2H, CH$_2$), 4.56-4.61 (m, 2H, CH$_2$), 6.48 (s, 1H, NH), 7.02-7.08 (m, 1H, CH$_{Ar}$), 7.26-7.41 (m, 5H, 5xCH$_{Ar}$), 7.48-7.51 (m, 1H, CH$_{Ar}$), 7.59-7.65 (m, 1H, CH$_{Ar}$), 7.90-7.93 (m, 1H, CH$_{Ar}$), 8.30 (s, 1H, CH) ppm. ^{13}C- NMR (75 MHz, CDCl$_3$): δ = 30.72, 38.80, 41.33, 43.73, 44.09, 45.30, 113.83, 120.26, 123.69, 124.15, 129.12, 131.05, 131.54, 132.25, 133.82, 138.69, 150.00, 154.96, 155.07, 168.72 ppm. HRMS (ESI): m/z [M+H]$^+$ calculated for $C_{22}H_{24}N_5O_3$ 406.18737, found 406.1864.

4-(3-(2-Oxobenzo[*d*]oxazol-3(2*H*)-yl)propanoyl)-*N*-phenylpiperazine-1-carboxamide (64)

3-(2-Oxobenzo[*d*]oxazol-3(2*H*)-yl)propanoic acid **63** (104 mg, 0.5 mmol) was dissolved in DMF (5 ml) and HOBt (76 mg, 0.5 mmol) and DCC (103 mg, 0.5 mmol) were added at 0°C. After stirring for 2 hours at 0°C, *N*-phenylpiperazine-1-carboxamide **16** (102 mg, 0.5 mmol) was added. The mixture was stirred overnight at room temperature. The resulting mixture was diluted with CH_2Cl_2 (20 ml) and washed with water (2×20 ml). The combined organic layers were dried over anhydrous Na_2SO_4 and concentrated *in vacuo*. The crude residue was purified by silica gel flash column chromatography (a mixture of diethylether and methanol in a ratio of 10:1 as mobile phase) to afford the title compound (170 mg, 86 %). Purity (Method B): 99.29 %. ^{1}H-NMR (300 MHz, CDCl$_3$): δ = 2.94 (t, *J* = 6.8 Hz, 2H, CH$_2$), 3.48-3.59 (m, 6H, 3xCH$_2$), 3.71-3.75 (m, 2H, CH$_2$), 4.26 (t, *J* = 6.8 Hz, 2H, CH$_2$), 6.59 (s, 1H, NH), 7.10-7.43 (m, 9H, 9xCH$_{Ar}$) ppm. ^{13}C-NMR (75 MHz, CDCl$_3$): δ = 31.10, 38.66, 41.33, 43.63, 44.00, 45.19, 109.20, 110.19, 120.28, 122.67, 123.65, 124.14, 129.09, 131.19, 138.73, 142.78, 154.96, 168.74 ppm.

4-(3-(2,3-Dihydro-4*H*-benzo[*b*][1,4]oxazin-4-yl)propanoyl)-*N*-phenylpiperazine-1-carboxamide (66)

A mixture of 3,4-dihydro-2*H*-benzo[*b*][1,4]oxazine **65** (67 mg, 0.5 mmol), DIPEA (0.24 ml, 1.4 mmol) and ethyl 3-bromopropionate (380 mg, 2.4 mmol) in DMF (3 ml) was stirred at 80°C for 48 hours. When the reaction was finished, the mixture was diluted with water (15 ml) and extracted with dichloromethane (3x10 ml). The organic phases were combined and washed with water (15 ml). The combined organic layers were dried over anhydrous Na_2SO_4 and evaporated *in vacuo*. The crude residue was dissolved in THF (5 ml) and a solution of LiOH (42 mg, 1 mmol) in water (5 ml) was added. The mixture was stirred for 18 hours at 60°C. Then, the pH was adjusted to 3 with 2N hydrochloric acid and the compound was extracted with ethyl acetate (3x20 ml). The combined organic layers were dried over anhydrous Na_2SO_4. After solvent evaporation, the pure acid compound was obtained. The acid was redissolved in DMF (5 ml), and HOBt (76 mg, 0.5 mmol) and DCC (103 mg, 0.5 mmol) were added at 0°C. After stirring for 2 hours, *N*-phenylpiperazine-1-carboxamide **16** (102 mg, 0.5 mmol) was added. The mixture was stirred overnight at room temperature. The resulting mixture was diluted with CH_2Cl_2 (20 ml) and washed with water (2×20 ml). The organic phase was dried over Na_2SO_4 and concentrated *in vacuo*. The crude residue was purified by silica gel flash column chromatography (using a mixture of diethylether and methanol in a ratio of 10:1 as mobile phase) to afford the title compound (96 mg, 49 %). Purity (Method A): 95.43 %. ^{1}H-NMR (300 MHz, CDCl$_3$): δ = 2.58-2.63 (m, 2H, CH$_2$), 3.37-3.50 (m, 8H, 4xCH$_2$), 3.65-3.70 (m, 4H, 2xCH$_2$), 4.20-4.23 (m, 2H, CH$_2$), 6.59 (s, 1H, NH), 6.60-6.67 (m, 2H, 2xCH$_{Ar}$), 6.77-6.86 (m, 2H, 2xCH$_{Ar}$), 7.02-7.07 (m, 1H, CH$_{Ar}$), 7.24-7.34 (m, 4H, 4xCH$_{Ar}$) ppm. ^{13}C-NMR (75 MHz, CDCl$_3$): δ = 29.39, 41.20, 43.55, 44.10, 45.27, 47.04, 47.67, 64.60, 111.81, 116.67, 117.82, 120.38, 121.83, 123.63, 129.04, 134.49, 138.74, 144.27, 155.03, 170.43 ppm.

14

FULL PAPER

Mycobacterial ThyX NADPH oxidase assay

M. tuberculosis ThyX was produced and purified as described.[18] The synthesized compounds were screened using a NADPH oxidation assay for *M. tuberculosis* ThyX activity in 96-well plates.[27] To determine IC_{50} values of compounds **22g**, **27**, **28**, **29d**, **45c**, **48** and **52,** the reaction mixture (100 µL) contained 50 mM HEPES pH7.5, 1mM $MgCl_2$, 12 µM FAD, 0.5% glycerol, 0.05% Triton X-100, 0.5 mg/mL BSA, 3 µM dUMP, 2.5% DMSO, a range of concentrations (ranging from 40 nM to 20 µM) of each testing compound and 0.5 µM of purified *Mtb*ThyX. After incubation of 15 min, the reactions were initiated by adding 600 µM NADPH and the decrease in absorbance at 340 nm was detected using CLARIOstar microplate reader (BMG Labtech) after 1 hour. The experiment was done in duplicates and repeated 3 to 4 times. In the control reactions, no enzyme or no inhibitor was used. Reported IC_{50} values were determined by normalizing the absorbance values to the control points and fitting the data to a Nonlinear Regression (dose response inhibition) using Graphpad Prism software.

To understand the detailed kinetic mechanisms involved in the interaction of the molecules with Mtb ThyX, the NADPH oxidase assay of ThyX enzyme was measured under various combinations of concentrations for compounds **22a, 22c, 22e, 22i** and **22k** (1-100 µM) and substrates concentrations. All molecules were solubilized in dimethylsulfoxide (DMSO) and used at a 1% final concentration of DMSO during the test. One hundred microlitres of standard reaction mixture contained HEPES 50 mM pH 8, NaCl 30 mM, FAD 50 µM, β-mercaptoethanol 100 µM, dUMP 100 µM, NADPH 250 µM, and 10 µM of purified *Mtb*ThyX. According to the experiments, dUMP, NADPH and CH_2H_4Folate were varied across 5–100 µM, 50–500 µM and 10–125 µM, respectively. Microtitre plates were prepared and transferred to the microplate reader Chameleon II (Hidex). The reactions were started by automatically injecting NADPH into individual wells and ThyX activity was determined by following a decrease in absorbance at 340 nm. Samples with added DMSO and enzyme-free reactions were used as positive and negative controls, respectively. The inhibition data were globally fitted to all possible kinetic models including competitive, noncompetitive and uncompetitive inhibition models.

NADPH oxidase assay with ThyX from other species

The same set of molecules was also evaluated as potential inhibitors of ThyX activity from other species (*H. pylori, PBcv-1, B. hermsi, C. trachomatis*) using the NADPH oxidase assay under standard reaction conditions with 50 or 200 µM of molecules in the reaction assay.

ThyX activity was also measured by a deprotonation of [5-^{3}H-dUMP] test, with measurement of the tritium release during the reaction.[14] Molecules were used in 1% DMSO final at the concentrations described above, and reactions were started by addition of 10 µM of ThyX and stopped after 25 min of incubation at 37°C.

Molecular Modelling

Prior to energy minimization, all complexes were neutralized by adding Na^+ ions and Cl^- together with TIP3P water solvation. After minimization, the system was gradually heated from 0 to 300 K over 50 ps, reaching solvent density after another 500 ps. During the following 20 ns simulation, coordinate trajectories were collected every 2 ps after which CPPTRAJ modules of AMBER 16 were implied for trajectories analyses.[28] The root-mean-square-deviation (RMSD) of protein backbone, compound **10** and folinic acid were computed. RMSD convergence was reached after 15 ns for both complexes. The MMGBSA module in AmberTools17 was used to calculate the Gibbs free energy after 20 ns simulation indicating protein affinity for compound **10** compared to folinic acid.

References:

[1] World Health Organisation. Global Tuberculosis Report 2017.

[2] L.G. Dover, G.D. Coxon, J. Med. Chem. 2011, 54, 6157–6165.

[3] K. Andries, P. Verhasselt, J. Guillemont, H.W. Göhlmann, J.M. Neefs, H. Winkler, J. Van Gestel, P. Timmerman, M. Zhu, E. Lee, P. Williams, D. de Chaffoy, E. Huitric, S. Hoffner, E. Cambau, C. Truffot-Pernot; N. Lounis, V. Jarlier, Science 2005, 307, 223-227.

[4] M.T. Gler, V. Skripconoka, E. Sanchez-Garavito, H. Xiao, J.L. Cabrera-Rivero, D.E. Vargas-Vasquez, M. Gao, M. Awad, S.K. Park, T.S. Shim, G.Y. Suh, M. Danilovits, H. Ogata, A. Kurve, J. Chang, K. Suzuki, T. Tupasi, W.J. Koh, B. Seaworth, L.J. Geiter, C.D. Wells, N. Engl. J. Med. 2012, 366, 2151-2160.

[5] D.T. Hoagland, J. Liu, R.B. Lee, R.E. Lee, 2016, 102, 55–72.

[6] C.W. Carreras, D.V. Santi, Annu. Rev. Biochem. 1995, 64, 721–762.

[7] H. Myllykallio, G. Lipowski, D. Leduc, J. Filee, P. Forterre, U. Liebl, Science 2002, 297, 105–107.

[8] a) T.V. Mishanina, L. Yu, K. Karunaratne, D. Mondal, J.M. Corcoran, M.A. Choi, A. Kohen, Science 2016, 29, 507-510. b) T.V. Mishanina, E.M. Koehn, J.A. Conrad, B.A. Palfey, S.A. Lesley, A. Kohen, J. Am. Chem. Soc. 2012, 134, 4442-4448. c) E.M. Koehn, A. Kohen, Arch. Biochem. Biophys. 2010, 493, 96-102.

[9] I. Mathews, A.M. Deacon, J.M. Canaves, D. McMullan, S.A. Lesley, S. Agarwalla, P. Kuhn, Structure 2003, 11, 677-690.

[10] a) A.S. Fivian-Hughes, J. Houghton, E.O. Davis, Microbiology 2012, 158, 2, 308-318. b) J. Rengarajan, B.R. Bloom, E.J. Rubin, Proc. Natl. Acad. Sci. U.S.A. 2005, 102, 8327–8332. c) C.M. Sassetti, D.H. Boyd, E.J. Rubin, Mol. Microbiol. 2003, 48, 77–84.

[11] M. Choi, K. Karunaratne, A. Kohen, Flavin-Dependent Thymidylate Synthase as a New Antibiotic Target. Molecules 2016, 21, 654.

[12] M. Kogler, B. Vanderhoydonck, S. De Jonghe, J. Rozenski, K. Van Belle, J. Herman, T. Louat, A. Parchina, C. Sibley, E. Lescrinier, P. Herdewijn, J. Med. Chem. 2011, 54, 4847–4862.

[13] T. Basta, Y. Boum, J. Briffotaux, H.F. Becker, I. Lamarre-Jouenne, J.C. Lambry, S. Skouloubris, U. Liebl, M. Graille, H. van Tilbeurgh, H. Myllykallio, Open Biol. 2012, 2, 120120.

[14] S. Skouloubris, K. Djaout, I. Lamarre, J.C. Lambry, K. Anger, J. Briffotaux, U. Liebl, H. de Reuse, H. Myllykallio, Open Biol. 2015, 5, 150015.

[15] J.L. Bolton, M.A. Trush, T.M. Penning, G. Dryhurst, T.J. Monks, Chem. Res. Toxicol. 2000, 13, 135-160.

[16] F. Esra Onen, Y. Boum, C. Jacquement, M.V. Spanedda, N. Jaber, D. Scherman, H. Myllykallio, J. Herscovici, Bioorg. Med. Chem. Lett. 2008, 18, 3628-3631.

[17] R. Luciani, P. Saxena, S. Surade, M. Santucci, A. Venturelli, C. Borsari, G. Marverti, G. Ponterini, S. Ferrari, T.L. Blundell, M.P. Costi, J. Med. Chem. 2016, 59, 9269-9275.

[18] R. Abu El-Asrar, L. Margamuljana, H. Klaassen, M. Nijs, A. Marchand, P. Chaltin, H. Myllykallio, H.F. Becker, S. De Jonghe, P. Herdewijn, E. Lescrinier, Biochem. Pharmacol. 2017, 135, 69–78.

[19] V. Rajachandrashekara, B.G. Vineela, S. Venkataiaha, P.K. Dubey, Der Pharma Chemica, 2014, 6, 7-10.

[20] D.S. Johnson, K. Ahn, S. Kesten, S.E. Lazerwith, Y. Song, M. Morris, L. Fay T. Gregory, C. Stiff, J.B. Dunbar Jr., M. Liimatta, D. Beidler, S. Smith, T.K. Nomanbhoy, B.J. Cravatt, Bioorg. Med. Chem. Lett. 2009, 19, 2865-2869.

[21] F.L. Atkinson, M.D. Barker, S.A. Campos, N.J. Parr, V.K. Patel, (Glaxo Group Ltd, Greenford Middlesex, GB), Int. PCT Pub. No. WO2006129100.

15

WILEY-VCH

FULL PAPER

[22]   R.E. TenBrink, W.B. Im, V.H. Sethy, A.H. Tang, D.B. Carter, J. Med. Chem. 1994, 37, 758–768.

[23]   E.M. Koehn, L.L. Perissinotti, S. Moghram, A. Prabhakar, S.A. Lesley, I.I. Mathews, A. Kohen, Proc. Natl. Acad. Sci. U S A. 2012, 109, 15722-15727.

[24]   P. Sampathkumar, S. Turley, J.E. Ulmer, H.G. Rhie, C.H. Sibley, W.G. Hol, J. Mol. Biol. 2005, 352,1091-1104.

[25]   D.A. Case, D.S. Cerutti, T.E. Cheatham III, T.A. Darden, R.E. Duke, T.J. Giese, H. Gohlke, A.W. Goetz, D. Greene, N. Homeyer, S. Izadi, A. Kovalenko, T.S. Lee, S. LeGrand, P. Li, C. Lin, J. Liu, T. Luchko, R. Luo, D. Mermelstein, K.M. Merz, G. Monard, H. Nguyen, I. Omelyan, A. Onufriev, F. Pan, R. Qi, D.R. Roe, A. Roitberg, C. Sagui, C.L. Simmerling, W.M. Botello-Smith, J. Swails, R.C. Walker, J. Wang, R.M. Wolf, X. Wu, L. Xiao, D.M. York, P.A. Kollman, AMBER 2017, 2017, University of California, San Francisco.

[26]   A. Marchler-Bauer, Y. Bo, L. Han, J. He, C.J. Lanczycki, S. Lu, F. Chitsaz, M.K. Derbyshire, R.C. Geer, N.R. Gonzales, M. Gwadz, D.I. Hurwitz, F. Lu, G.H. Marchler, J.S. Song, N. Thanki, Z. Wang, R.A. Yamashita, D. Zhang, C. Zheng, L.Y. Geer, S.H. Bryant, Nucleic Acids Res. 2017. 45(D1):D200-D203.

[27]   K. Djaout, V. Singh, Y. Boum, V. Katawera, H.F. Becker, N.G. Bush, S.J. Hearnshaw, J.E. Pritchard, P. Bourbon, P.B. Madrid, A. Maxwell, V. Mizrahi, H. Myllykallio, S. Ekins, Sci. Rep. 2016, 10, 27792.

[28]   D.R. Roe, T.E. Cheatham III, J. Chem. Theory Comput. 2013, 9, 3084–3095.

Entry for the Table of Contents

29d: *Mbt* ThyX IC$_{50}$ = 0,69 µM
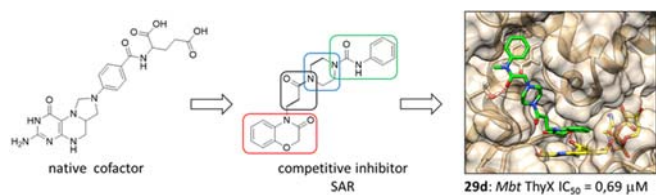
Starting from a previously identified mycobacterial ThyX inhibitor based on a benzo[b][1,4]oxazin-3(4H)-one scaffold, a systematic structure-activity relationship study was performed. It led to the discovery of a benzo[b][1,4]oxazin-3(4H)-one analogue displaying an IC$_{50}$ value of 0.69 µM. These heterocycles can be used as starting points for the discovery of novel antibacterial agents acting via ThyX inhibition.